

# **Human Perception of Ambiguous Inertial Motion Cues**

**Guan-Lu Zhang**

Individual Project Report submitted to the International Space University in partial fulfillment of the requirements of the M.Sc. Degree in Space Studies

**August 2010**

Internship Mentor: **Dr. Scott Wood and Dr. Gilles Clément**

Host Institution: **Neuroscience Laboratory, NASA JSC, Houston, Texas**

ISU Academic Advisor: **Prof. John Farrow**

## **Acknowledgement**

Firstly, I am extremely thankful for Dr. Scott Wood's support and guidance as my mentor at the Neuroscience lab. I am also grateful that Dr. Gilles Clément introduced me to the space life science field during my studies at the International Space University. My internship at NASA JSC would not be possible without the efforts of Dr. Wood, Ms. Janet Cook and Ms. Judith Hayes during the badging process. Finally, I would like to thank all of my colleagues at the Neuroscience lab for their advice and support during the course of my internship.

## **Abstract**

Human daily activities on Earth involve motions that elicit both tilt and translation components of the head (i.e. gazing and locomotion). With otolith cues alone, tilt and translation can be ambiguous since both motions can potentially displace the otolithic membrane by the same magnitude and direction. Transitions between gravity environments (i.e. Earth, microgravity and lunar) have demonstrated to alter the functions of the vestibular system and exacerbate the ambiguity between tilt and translational motion cues. Symptoms of motion sickness and spatial disorientation can impair human performances during critical mission phases. Specifically, Space Shuttle landing records show that particular cases of tilt-translation illusions have impaired the performance of seasoned commanders. This sensorimotor condition is one of many operational risks that may have dire implications on future human space exploration missions.

The neural strategy with which the human central nervous system distinguishes ambiguous inertial motion cues remains the subject of intense research. A prevailing theory in the neuroscience field proposes that the human brain is able to formulate a neural internal model of ambiguous motion cues such that tilt and translation components can be perceptually decomposed in order to elicit the appropriate bodily response. The present work uses this theory, known as the GIF resolution hypothesis, as the framework for experimental hypothesis. Specifically, two novel motion paradigms are employed to validate the neural capacity of ambiguous inertial motion decomposition in ground-based human subjects. The experimental setup involves the Tilt-Translation Sled at Neuroscience Laboratory of NASA JSC. This two degree-of-freedom motion system is able to tilt subjects in the pitch plane and translate the subject along the fore-aft axis. Perception data will be gathered through subject verbal reports.

Preliminary analysis of perceptual data does not indicate that the GIF resolution hypothesis is completely valid for non-rotational periodic motions. Additionally, human perception of translation is impaired without visual or spatial reference. The performance of ground-base subjects in estimating tilt after brief training is comparable with that of crewmembers without training.

## Table of Contents

Acknowledgement .....	ii
Abstract.....	iii
List of Figures.....	v
Nomenclature.....	vi
1 Introduction.....	1
1.1 Human Vestibular Organ .....	3
1.2 Previous Work .....	7
1.3 Purpose of the study.....	9
1.4 Hypothesis.....	10
2 Experimental Details.....	11
2.1 Test-bed Description.....	11
2.2 Methods.....	12
2.3 Experimental Procedures .....	13
2.4 Motion Profiles .....	15
2.5 Data Collection Methods .....	21
3 Considerations for Human Subject Testing .....	22
3.1 Risk and Hazards Analysis .....	23
4 Results.....	27
4.1 Tilt and Translation Calibrations .....	27
4.2 Effects of Training in Tilt .....	28
4.3 Effects of Training in Translation.....	29
4.4 Dynamic Tilt Perception.....	31
4.5 Dynamic Translation Perception.....	32
4.6 Axis of Rotation Locations .....	33
4.7 Resultant Acceleration Analysis .....	35
5 Discussion.....	40
6 Works Cited .....	41
Appendix.....	42

## List of Figures

Figure 1: Interior of the Lunar Module.....	2
Figure 2: Principal Structures of the Human Vestibular System.....	3
Figure 3: Principal Planes and Axes of the Human Body .....	5
Figure 4: Bode Plots of Semicircular Canal .....	6
Figure 5: Principal of Equivalent Accelerations.....	6
Figure 6: Frequency Response of Vestibulo-Ocular Reflex.....	7
Figure 7: Schematic for Multisensory Integration.....	8
Figure 8: GIF Resolution Hypothesis .....	9
Figure 9: ZIG – ZAG Hypothesis .....	10
Figure 10: Head Centered Coordinate Frame .....	12
Figure 11: TTS Exterior.....	12
Figure 12: TTS Interior.....	12
Figure 13: Tilt Perception Training .....	14
Figure 14: Tilt Perception Calibration .....	14
Figure 15: Translation Perception Training Profile.....	14
Figure 16: Translation Perception Calibration Profile.....	15
Figure 17: Acceleration Vector of Tilt Sines.....	16
Figure 18: Acceleration Vector of Translation Sines .....	17
Figure 19: Acceleration Vectors of ZIG Sines .....	18
Figure 20: Acceleration Vectors of ZAG Sines.....	19
Figure 21: Z-Axis Independent Gravitoinertial (ZIG) Motion Profile .....	20
Figure 22: Z-Axis Aligned Gravitoinertial (ZAG) Motion Profile.....	20
Figure 23: Locations of Perceived Rotation Axis.....	21
Figure 24: Pre Risk Mitigation Assessment.....	23
Figure 25: Post Risk Mitigation Assessment.....	23
Figure 26: Tilt Perception Calibration .....	27
Figure 27: Translation Perception Calibration.....	28
Figure 28: Static Tilt Perception: Control vs. Crewmembers.....	29
Figure 29: Static Translation Perception.....	30
Figure 30: The Aubert – Müller Effect.....	30
Figure 31: Dynamic Tilt Perception .....	32
Figure 32: Dynamic Translation Perception.....	33
Figure 33: Rotation Axis Locations.....	34
Figure 34: Absolute Difference in Rotation Axis Locations .....	35
Figure 35: Perceived Accelerations When Rotation Axis is Above the Head.....	36
Figure 36: Perceived Accelerations When Rotation Axis is Below the Head.....	37
Figure 37: Resultant Acceleration Analysis .....	39

## **Nomenclature**

HRP	Human Research Program
JSC	Johnson Space Center
ISS	International Space Station
CNS	Central Nervous System
LM	Lunar Module
PIO	Pilot Induced Oscillations
VOR	Vestibulo-Ocular Reflex
OCR	Ocular Counter-Rolling
GIF	Gravito-Inertial Force
ZIG	Z-Axis Independent Gravitoinertial Motion
ZAG	Z-Axis Aligned Gravitoinertial Motion
TTS	Tilt-Translation Slide
OEC	On-board Embedded Controller
PID	Proportional Integral Derivative
DVR	Digital Video Recorder
CPHS	Committee for the Protection of Human Subjects
EOT	End-of-Travel
SEM	Standard Error Mean
NFPA	National Fire and Protection Association
IREDD	Infrared Emitting Diodes
ACGIH	American Conference of Governmental Industrial Hygienists

## **1 Introduction**

In October of 2005, the Human Research Program (HRP) was established at the NASA Johnson Space Center (JSC) in order to investigate and mitigate risks to human health and performance in space exploration missions. One of the risks is the impaired control of spacecraft due to altered sensorimotor functions associated with spaceflight. Although not all crewmembers have shown symptoms of altered perception, postural and locomotor control, the possibility of impaired alteration on the human vestibular system is of interest for future Mars missions and current missions to and from the International Space Station (ISS).

Manual control of vehicles and other complex systems is a critical element of any human spaceflight mission. The task demands the human operator to integrate many high-level functions of the central nervous system (CNS). These tasks require the effective performance of motion perception, dynamic visual acuity, hand-eye coordination and cognitive function. As the fundamental orientation reference, the gravity vector is sensed by the vestibular, proprioceptive and kinesthetic receptors, and used by the CNS to orient and navigate the body. Disturbances of this orientation reference, either due to ototoxic diseases or due to gravity transitions during spaceflight, can lead to impaired awareness in self-orientation and deficit in movement coordination.

Specifically, transitions between various gravity environments (i.e. Earth, microgravity and lunar) have demonstrated to alter the functions of the vestibular system causing symptoms of motion sickness and spatial disorientation among astronauts. Russian Cosmonaut Gherman Stepanovich Titov, the second human in space, reported to have experienced the inversion illusion, i.e., the sensation of “hanging upside down,” immediately after exposure to weightlessness (CLÉMENT, G. and Reschke, M. F., 2008). Novel environment conditions such as lunar dust blowback have challenged the crews of Apollo by impairing visibility. While piloting the Apollo Lunar Module (LM) during descent, many commanders chose to fly manually even though the fully automatic landing capability was available. Through the window reticle of the LM (see Figure 1), commanders designated landing spots visually, while another astronaut verbally stated vehicle parameters. Without electronic map or landing profile displays, many had problems recognizing landmarks, sensing vehicle attitude and estimating distances due to the ambiguity of terrain features in the mist of airborne lunar dust. Specifically, Apollo 11 and 12 crews attributed dust blowback to difficulty in nulling motion disturbances during landing (PALOSKI, W.H. et al., 2008).

Despite intensive training on shuttle commanders and pilots, some landings have exhibited non-desirable performance due to momentary spatial disorientation after re-entry. One of the prevailing misperceptions is the tilt-translation illusion, which involves incorrect estimation of tilt angle or inability to distinguish tilt from translation. During the landing of STS-3 mission in

1982, the commander took over manual control of the shuttle 30 seconds before touchdown. The shuttle exhibited three full cycles of pilot induced oscillations (PIO) with increasing amplitude. No anomaly was discovered in the flight control system during post-flight analysis but evidence from flight data showed five amplitude reversals in the pitch plane. It is plausible that the commander underestimated the pitch angle due to tilt-translation ambiguities and induced the PIO to overcompensate the misperception (PALOSKI, W.H. et al., 2008).



**Figure 1: Interior of the Lunar Module**  
Photo courtesy of the Franklin Institute

These conditions are operational risks that may have dire implications on future human space exploration missions. One of the critical phases of an exploration class mission is landing the crew vehicle. Despite the presence of automated systems, astronauts are expected to be in-the-loop or perhaps assume complete manual control for tasks such as re-designate the landing site, modify descent trajectory and maintain vehicle attitude. While in manual takeover, various visual and vestibular stimuli could evoke powerful illusions that quickly lead to loss of control of the vehicle. The neuroscience research community plays an important role in understanding the mechanisms of motion perception within the human brain and in developing countermeasures in all aspects of mission design in order to facilitate crew safety and wellbeing.

## 1.1 Human Vestibular Organ

The vestibular system is the human equivalent of the inertial navigation unit of a spacecraft. Its main purpose is to detect orientation and motion changes without external references cues such as visual or somatosensory signals. Two types of end-organs make up the human vestibular system: one transduces angular acceleration (i.e. semi-circular canals) and the other transduces linear acceleration (i.e. otoliths). Figure 2 illustrates the morphology of the inner ear in diagrammatic form. It is clear that there are anatomical and functional differences between the three orthogonally oriented semi-circular canals and the two perpendicularly oriented otoliths. The membranous labyrinth, which contains the vestibular end-organs and the spiraling cochlea, which contains the hearing organ, both share the same contoured cavity of the bouldered temporal bone. They are interconnected by the endolymph fluid. Both the labyrinth and the cochlea transmit afferent signals to the CNS via the eighth cranial nerve (BENSON, A.J., 1982).

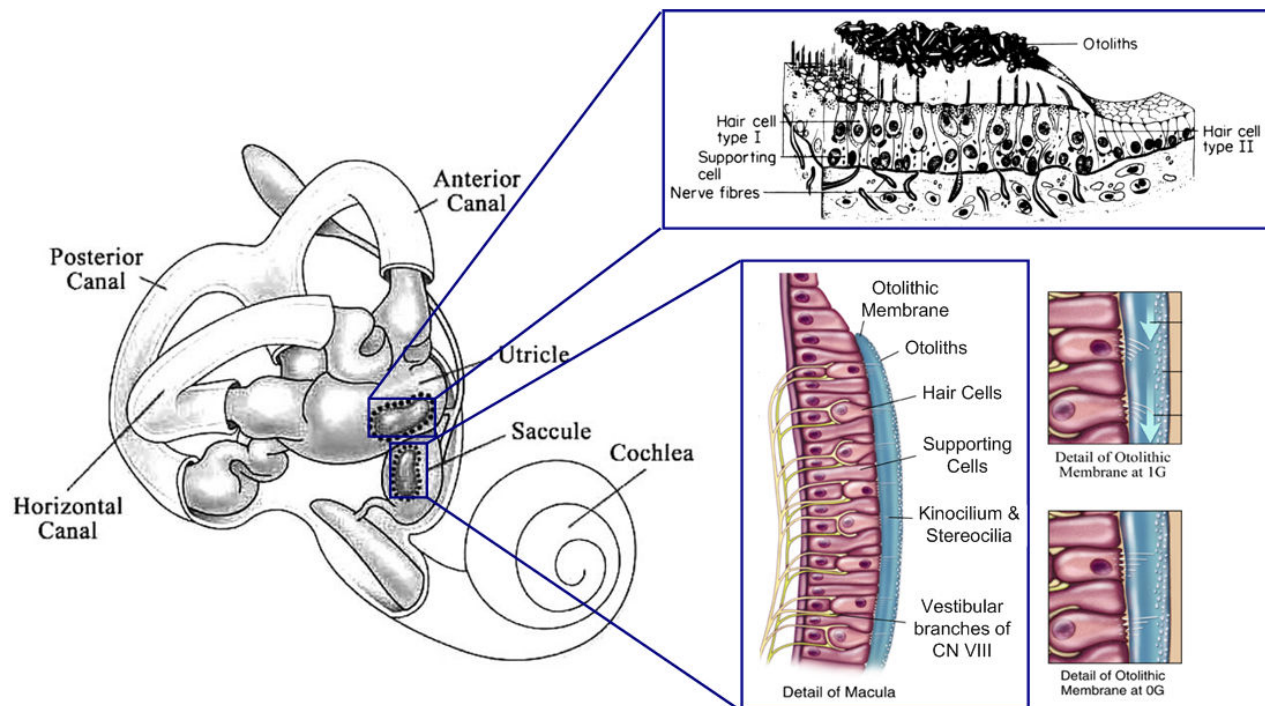


**Figure 2: Principal Structures of the Human Vestibular System**  
Illustration courtesy of Clément & Hamilton (2003)

The three semi-circular canals are identified as anterior, posterior and lateral. On average, the local plane of the human head on which the lateral canal occupies becomes co-planar with the world horizon when the head tilts forward approximately 30 degrees. The anterior and posterior canals are approximately vertical and they are mutually oriented about 45 degrees with respect to the sagittal and coronal planes. Figure 3 illustrates principal planes, axes and attitude directions

of the human coordinate system. A fluid called endolymph fills the interconnecting canals and each canal has an enlarged terminal at its base called the ampulla. When the head experiences angular acceleration, the inertial motion of endolymph deflects hair cells at the base of ampulla and transduces the signal via the vestibular nerve to the brain. Collectively, the canals indicate rotations about three axes: roll, pitch and yaw. Previous work by Goldberg and Fernandez (1971) examined the frequency response of squirrel monkey semicircular canals. Their results (see Figure 4) indicate that the sensitivity of canals diminish drastically below 0.1Hz and the phase error (i.e. lead) progressively increases with decreasing frequency in the same region. The corner frequency of 0.1Hz can be approximated as the reference frequency of ideal canal response for humans.

The two otoliths are identified as the utricle and the saccule, which is for the horizontal and vertical directions, respectively. Each otolith organ consists of two main parts, the macula and the otolithic membrane. The macula is the base structure on the bony labyrinth that includes hair cells that transmit signals upon deflections from the otolithic membrane. The membrane is a gelatinous substance that displaces in shear when the head experiences linear acceleration. Given this mechanism of transduction, tilt and translation are motion cues particularly deceptive without the presence of visual feedback. These motions are ambiguous to the human vestibular organ because the displacements in shear are fundamentally equivalent between tilt and translation as noted by Einstein. The Einstein equivalence principle states that, on Earth, linear acceleration and tilt with respect to gravity are indistinguishable for all linear accelerometers. In other words, with otolith cues alone, tilt and translation can be ambiguous since both motions can potentially displace the otolithic membrane by the same magnitude and direction. Figure 5 provides an illustrative example of this principle.

Of the many techniques to gather data on human vestibular afferent signals and motion perceptions, few are ethically acceptable in their invasive nature and experimentally convenient in their procedural complexity. The most common techniques practiced by neuroscience researchers are tracking the vestibulo-ocular reflex (VOR), monitoring the performance of manual tasks and asking subjects to report perception in quantitative measures (i.e. angles or distances) or through qualitative means (i.e. drawing motion profiles). VOR is the compensatory eye movement elicited by stimulation of the otolith organs. From studying animals, it is known that this reflexive motor response is present with the removal of the cerebrum. Hence, observing VOR in human subjects is particularly effective as a research technique because the experimental setup (i.e. infrared video oculography) is relatively easy to implement and it bypasses the cognitive functions of CNS, which may often bring variability among subject verbal reports. The drawback of VOR is that it is not observable in all directions of motion. For example, linear fore-aft motions do not produce noticeable changes in ocular position nor orientation. In such cases, verbal reports and manual tasks to indicate perception of linear translation must be utilized.

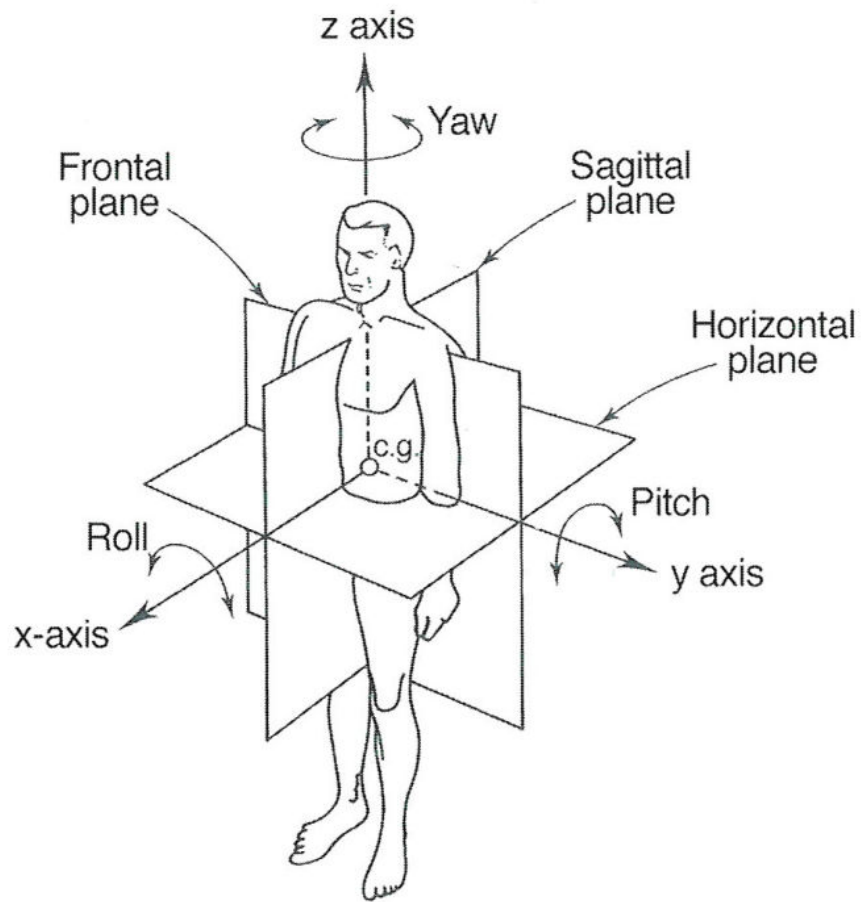


**Figure 3: Principal Planes and Axes of the Human Body**  
Illustration courtesy of Clément and Reschke (2008)

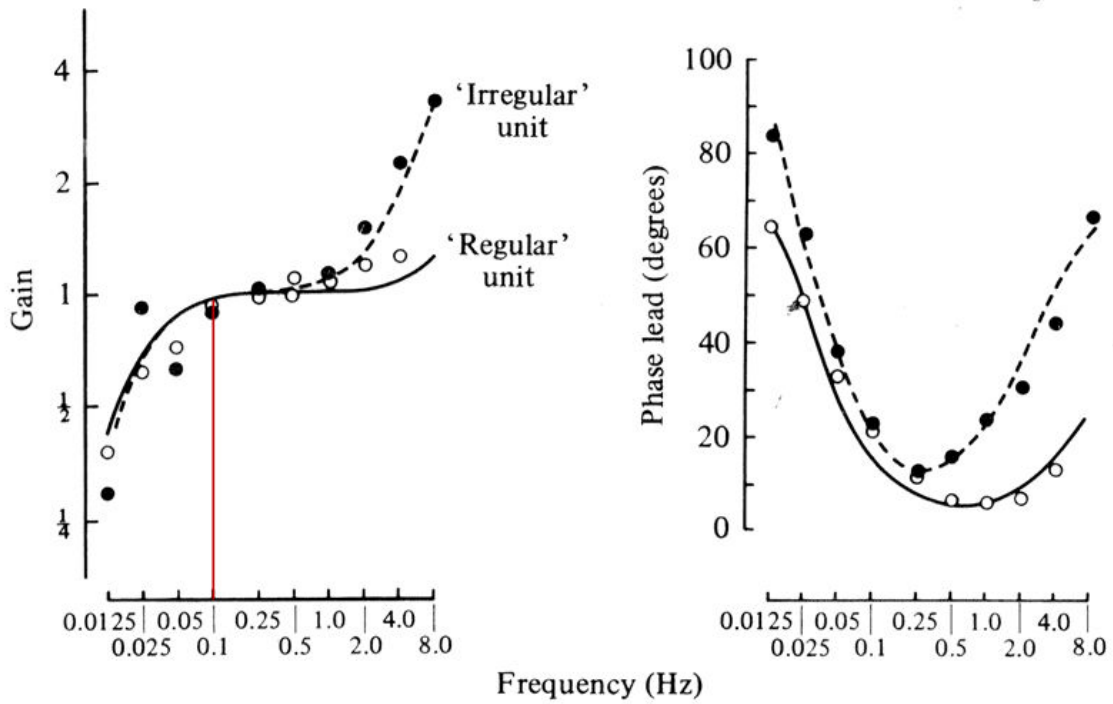


**Figure 4: Bode Plots of Semicircular Canal**  
 Figure adapted from Benson (1982)

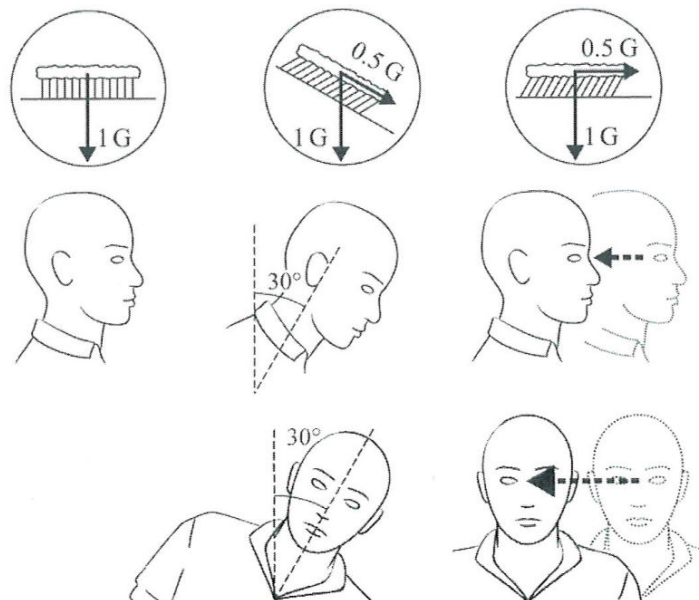


**Figure 5: Principal of Equivalent Accelerations**  
 Illustration courtesy of Clément and Reschke (2008)

## 1.2 Previous Work

Neuroscience investigators have proposed many theories as an effort to understand the mechanism with which the CNS uses to differentiate ambiguous tilt and translation cues. These theories generally fall into two classifications: frequency segregation and multisensory integration.

The frequency segregation hypothesis claims that the perceptual responses to tilt and translation are fundamentally differentiated as a function of stimulus frequency. As described in the previous section, a widely practiced technique is the examination of the ocular response to motion stimuli. When the head is tilted in periodic fashion, both eyes instinctively rolls accordingly in the opposite direction. This reflex response is known as ocular counter-rolling (OCR). Similarly, when the head is rotated about its z-axis, both eyes undergo saccadic return movements leading to optokinetic nystagmus. As a measure of quantifying the VOR, the gain is calculated as the ratio of eye movement with respect to head movement. Figure 6 illustrates the frequency response of the VOR using data from works of Paige & Seidman (1999) and Wood (2002). It is evident that during low frequency motion, the perception of tilt is most dominant as indicated by gain values close to unity. As frequency increases, tilt perception gradually diminished as translation perception steadily approaches unity. In other words, the human CNS interprets low frequency linear acceleration as tilt and high frequency linear accelerations as translation. In the cross over frequency range, between 0.3 and 0.4 Hz, the perception of the two motions becomes most ambiguous and this is a region where filtering is the least deterministic.

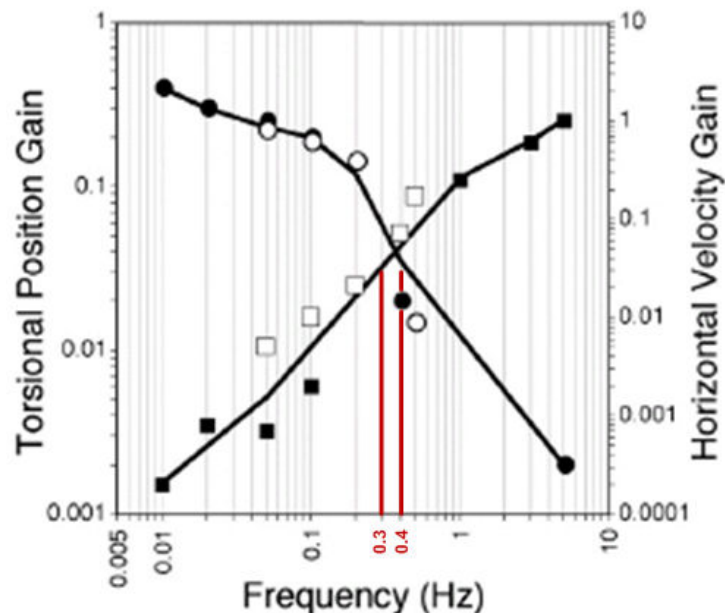


**Figure 6: Frequency Response of Vestibulo-Ocular Reflex**  
Figure adapted of Clément and Reschke (2008)

Alternatively, the multisensory integration hypothesis asserts that brain combines signals from the otoliths, the canals and vision to distinguish between head translation and tilt. Specifically, the brain creates an internal model of the motion where efferent and afferent are fused together to decipher ambiguity in sensory perceptions. This concept of neural representation of physical motion parameters would not have frequency dependence according to its advocates. Figure 7 illustrates the computational strategy used by the CNS to transform primary vestibular signals to physical motion parameters. Semicircular canal signals, which indicates angular velocity, are used to discriminate otolith signals into either orientation (i.e. tilt) or translation components. Orientation relative to gravity, in turn, is used to transform angular velocity with respect to the head to angular velocity with respect to the world (ANGELAKI, D. E. et al., 1999). Although the frequency segregation and multisensory integration are commonly established to be opposing concepts, they are not mutually exclusive. Clearly, multisensory integration is critical in the cross over frequency range where motion cues are most ambiguous but this neural strategy must also contribute significantly in the extreme frequency ranges where one end-organ is less accurate than the other as an accurate transducer of acceleration.

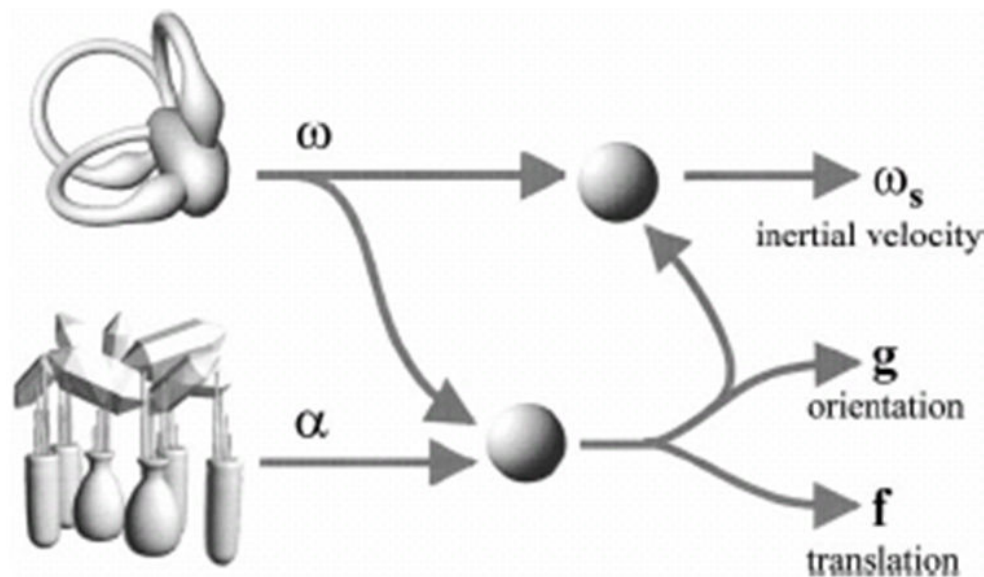


**Figure 7: Schematic for Multisensory Integration**  
**Illustration courtesy of Angelaki (1999)**

One specific example of the multisensory integration theory is the gravito-inertial force (GIF) resolution hypothesis formulated by Merfeld (1999). The fundamental idea of GIF resolution hypothesis is that given a force vector sense by the human vestibular system, the brain is able to decouple tilt and translation components and provide appropriate bodily responses to these motion cues. More importantly, as the sensation of tilt increases (i.e. approaching vertical), the

sensation of translation should decrease accordingly. Figure 8 illustrates this concept by rotating a subject about the z-axis horizontally. In a clock-wise rotation, the gravity vector,  $G$ , would point vertically down. According to Merfeld, the gravity vector is the GIF resultant vector  $\hat{F}$ . The instantaneous vector of tilt  $\hat{G}$  sensed by the vestibular system would be displaced by some degrees relative to the vertical. As a result, the human neural representation estimates a linear acceleration  $\hat{A}$  such that  $\hat{F} = \hat{G} - \hat{A}$ . As the subject continues in clock-wise rotation, neural estimate of tilt  $\hat{G}$  would increase and approach the resultant GIF. Consequentially, the neural estimate of linear translation would decrease given that the GIF remains constant as 1-g environment on Earth (MERFELD, D. et al., 1999).

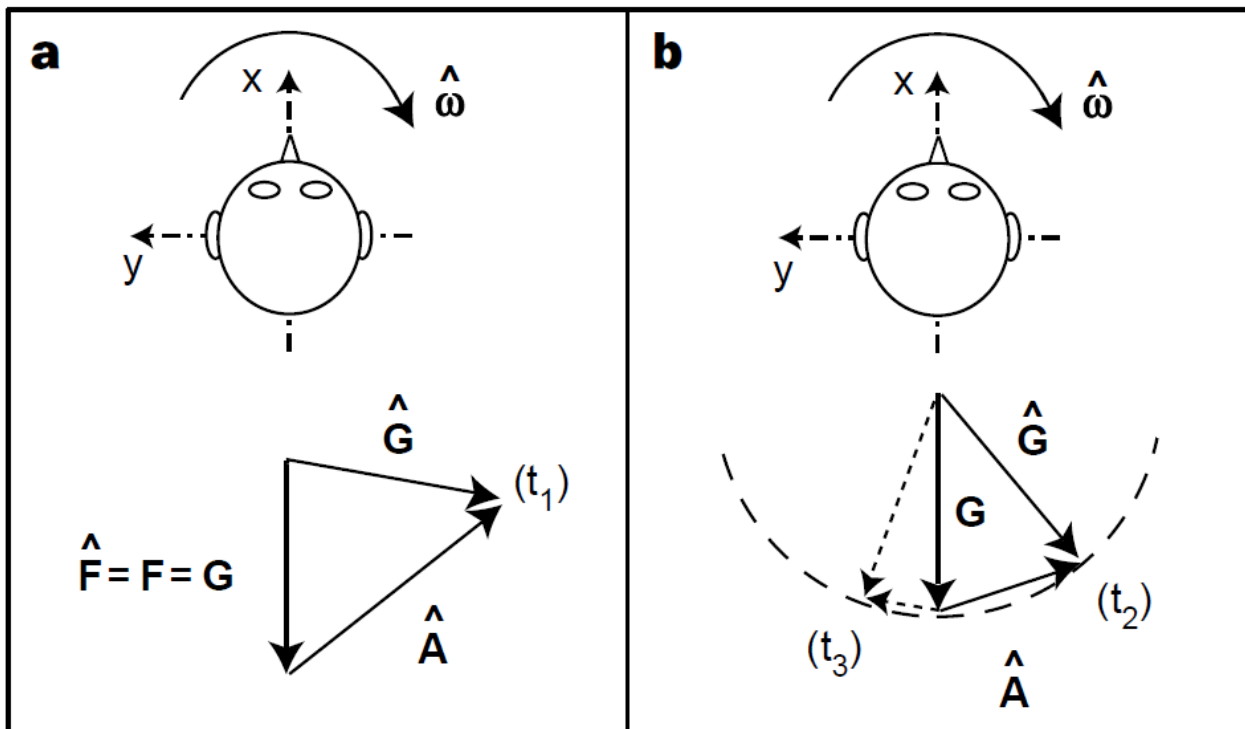


**Figure 8: GIF Resolution Hypothesis**  
**Illustration courtesy of Merfeld (1999)**

### 1.3 Purpose of the study

This study intends to characterize human perception of tilt and translation motions in the most ambiguous frequency of 0.3Hz. Specifically, this study aims to verify if the GIF resolution hypothesis is true for periodic motions in the pitch plane. The results of this study will be subsequently used to better understand the relationship between perceptual illusions evoked during passive motion and the performance parameters during manual control tasks.

Through the different combinations of tilt and translation motion profiles, two distinct motion paradigms are formulated to address the purpose of this study. The Z-axis Independent Gravito-inertial (ZIG) motion paradigm sums the two motions additively such that tilt and translation motions increases the angle of the resultant vector relative to the body z-axis. Conversely, the Z-axis Aligned Gravito-inertial (ZAG) motion paradigm sums the two motions such that tilt and translation motions mutually oppose each other and keeps the resultant vector aligned with the body z-axis. As control, motion paradigms with individual tilt and translation stimuli with varying amplitude will be employed. Finally, this study also intends to introduce a method of training on the perception of angular and linear displacements in order to enhance the accuracy of neural estimates for physical parameters.

#### 1.4 Hypothesis

The primary hypothesis of this study is that the ZIG paradigm will induce the perceptions of increased tilt and decreased translation compared with tilt only paradigm. Alternatively, the ZAG paradigm will induce the perceptions of increased translation and decreased tilt compared with translation only paradigm. Figure 9 illustrates the two elements of the hypothesis with vector diagrams on progressive phases of motion for each paradigm. The secondary hypothesis is that brief training in angular and linear displacements will assist subjects to more accurately perceive tilt and translational motion cues.

### Z-Axis Independent Gravito-inertial (ZIG) Motion      Z-Axis Aligned Gravito-inertial (ZAG) Motion

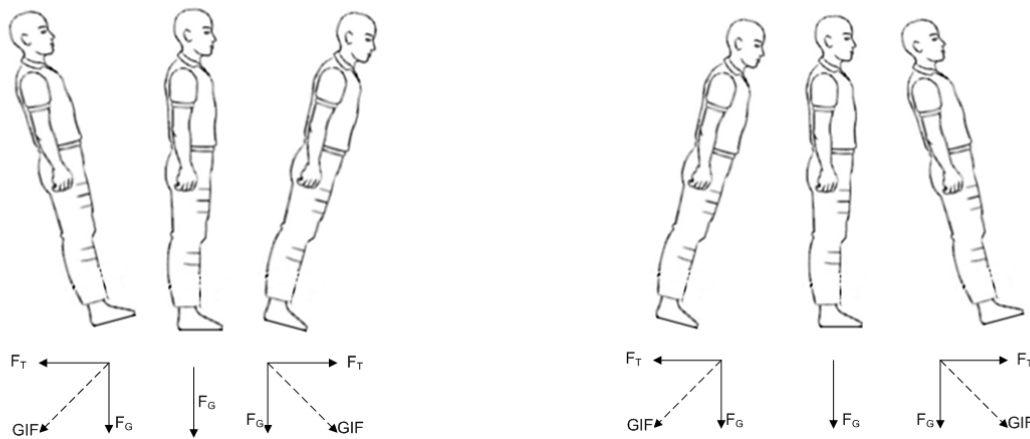


**Figure 9: ZIG – ZAG Hypothesis**  
**Illustrations adapted from Clément & Reschke (2008)**

## 2 Experimental Details

### 2.1 Test-bed Description

The Tilt-Translation Sled (TTS) is a two degree-of-freedom mechanism that is capable of inducing tilt and translation motions individually or both motions simultaneously. Specifically, the TTS can translate the subject in the fore-aft direction and orient the subject about the pitch plane. The translation motion along the air bearing track is provided by three linear motors operated in series on a single magnetic track. Compressed air (i.e. 90 psi) supports the seating enclosure at four points, allowing it to translate on the leveled epoxy surface nearly without friction. The approximate dimensions of the seating compartment are 1.85 meters in width, 2.45 meters in height and 2.25 meters in depth. A precision linear encoder provides accurate feedback for motion control and stability. A pneumatic driven anchor can be deployed to support subject ingress and egress. The tilt motion is generated by double friction wheels employing direct drive servo motors and a pivoting yoke assembly to induce  $\pm 20^\circ$  of maximum dynamic displacement and  $\pm 45^\circ$  of maximum static displacement.

The TTS control system comprises of a control console computer, on-board embedded controller (OEC) and relay-based safety subsystems. Data acquisition, motion control and safety subsystem interface are facilitated by National Instruments LabVIEW Real-Time Operating System. All drives are operated in torque mode using the standard Proportional Integral Derivative (PID) control scheme with position as the feedback parameter. In addition to two-way audio communication and infrared video surveillance, the control console includes a dedicated emergency stop switches that is independent of the OEC and console computer.

The subject is restrained in a modified performance vehicle seat via a five-point harness and the interaural axis of each subject (i.e. Y-axis in Figure 10) is adjusted to align with the rotation axis of the tilting seat (see Figure 12). This procedure is to ensure that each subject's vestibular system is isolated with the best effort in order to reduce eccentric stimulation of the inner ear organs. A one-degree-of-freedom potentiometer joystick is located on the subject's right side and the purpose of this instrument will be described in section 2.4. All visual and audio cues are removed from the subject in the dark enclosure and noise reducing head-phones. During the experimental session, the subject is able to communicate with the operators via microphone and headset. The operators are also able to monitor the subject inside the enclosure via infrared cameras. Each session with the subject is recorded on to a Digital Video Recorder (DVR) media as a backup data collection system.

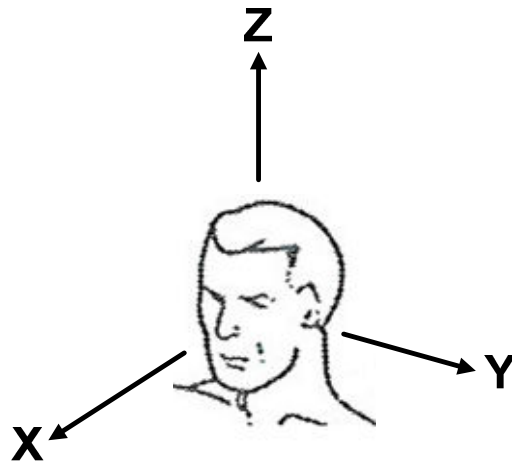


**Figure 10: Head Centered Coordinate Frame**  
Illustration adapted from Clément & Reschke (2008)



**Figure 11: TTS Exterior**



**Figure 12: TTS Interior**

## 2.2 Methods

A total of 12 ground based subjects between the ages of 23 and 61 (8 males and 4 females) with no history of vestibular disorders participated in this study. All subjects passed the U.S. Air Force Class III Flight Physical Exam. Before each session, a pre-test questionnaire was given to subjects in order to determine each person's susceptibility to motion sickness and overall state of

health on the day of the experiment. Experiences in piloting aircrafts were also included for future data analysis considerations. The subjects were also briefed on the experimental procedures with particular emphasis on the content of verbal report and tasks during the experiment. During the experiment, the operator periodically asked the subject to rate his or her sensation of nausea on a scale of 0 to 10, with 0 being normal and 10 being extremely nauseous. Although rating one's own state of nausea is quite subjective, the operators would stop all motions immediately when the nausea rating reaches 4 or 5. The subject may choose to take a break from the testing environment and resuming the experiment is absolutely voluntary. The intent of the study was only revealed to the subjects upon the completion of the experimental session.

### 2.3 Experimental Procedures

The study consists of two parts; one focuses on the subject's perception of head tilt and other on the perception of head translation. Each part consisted of the same set of six motion profiles, which will be described in detail in the next section. The order in which each part (i.e. tilt or translation) and the motion profiles within each set are presented to the subject is pseudo-randomized to avoid order effects during the investigation. Table 1 summarizes the experimental procedures and an example of the worksheet used in each experimental session is available in the Appendix.

**Table 1: Summary of Experimental Procedures**

		<b>Manual Task</b>	<b>Verbal Perception Report</b>	
<b>Tilt Perception</b>	<b>Training</b>	N/A	N/A	
	<b>Calibration</b>			
	<b>Tilt Sines 10°</b>	Mimic head tilt with joystick	Angular Displacements	Axis of Rotation
	<b>Tilt Sines 20°</b>			
	<b>Translation Sines 49cm</b>			
	<b>Translation Sines 100cm</b>			
	<b>ZIG Sines 10° 49cm</b>			
	<b>ZAG Sines 10° 49cm</b>			
<b>Translation Perception</b>	<b>Training</b>	N/A	N/A	
	<b>Calibration</b>			
	<b>Tilt Sines 10°</b>	Mimic head translation with joystick	Peak-to-Peak Displacement	
	<b>Tilt Sines 20°</b>			
	<b>Translation Sines 49cm</b>			
	<b>Translation Sines 100cm</b>			
	<b>ZIG Sines 10° 49cm</b>			
	<b>ZAG Sines 10° 49cm</b>			

Before presenting each set of the motion profiles, training and calibration of the subject's perception for tilt and translation were performed. The training is intended to allow the subject to become accustomed to the various angular and linear displacements. This adaptation would be helpful for the manual task of replicating the perceived motion and provide a reference for the perceived displacements. Specifically during training, subjects were informed of their angular orientation by the operator after each discrete movement in tilt training profile (see Figure 13). Subsequently in the calibration portion, each subject was asked to report his/her perceived angular displacement after the operator has indicated the completion of each discrete movement (see Figure 14). The intent of the calibration is to evaluate the effectiveness of the training and to normalize the perception among subjects. The same method is applied to the translation perception part, which trains and calibrates each subject's linear displacement (see Figure 15 and Figure 16). The displacement values for both profiles are slightly different from training to calibration in order to avoid training bias. The intent is to allow the CNS to establish a strategy of estimating the body position and then extrapolate this strategy on a new orientation or displacement.

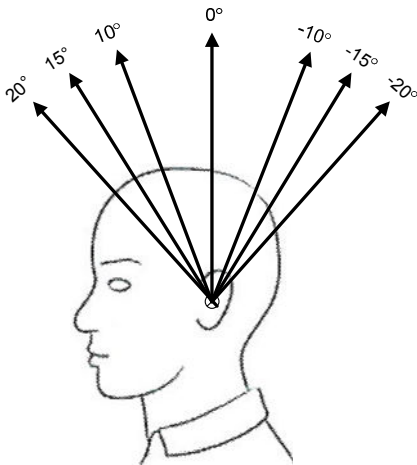


**Figure 13: Tilt Perception Training**

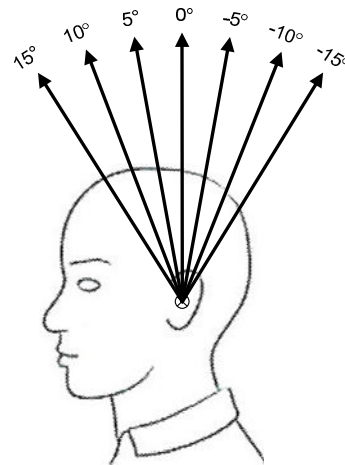


**Figure 14: Tilt Perception Calibration**

Illustrations adapted from Clément & Reschke (2008)

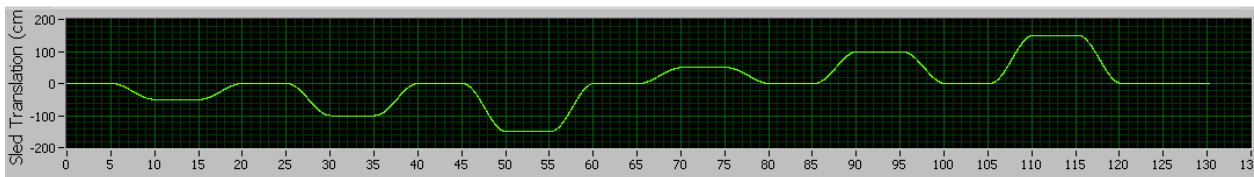


**Figure 15: Translation Perception Training Profile**

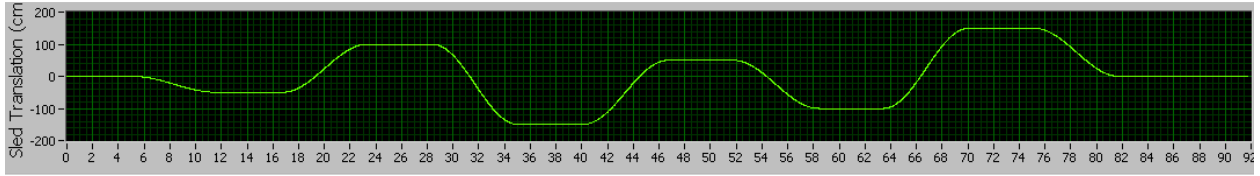


**Figure 16: Translation Perception Calibration Profile**

## 2.4 Motion Profiles

As previously mentioned, this study includes six motion paradigms. Each subject experiences the same set of profiles for the tilt perception and for the translation perceptions (see Table 1). Tilt sines  $10^\circ$  and  $20^\circ$  are purely sinusoidal motions in tilt with 10 and 20 degrees in amplitude (i.e.  $\theta_c$ ) respectively. The angular position with respect to time can be expressed by equation 1 and the magnitude of maximum acceleration in units of Earth gravity is expressed by equation (2). Figure 17 illustrates the actual location of the acceleration vector relative to the human interaural axis.

$$\theta(t) = \theta_c \sin(\omega t) \quad (1)$$

where:  $\omega = 2\pi f$

$$a_{TILT-X} = a_G \sin \theta_c \quad (2)$$

where:  $a_G = 1g$

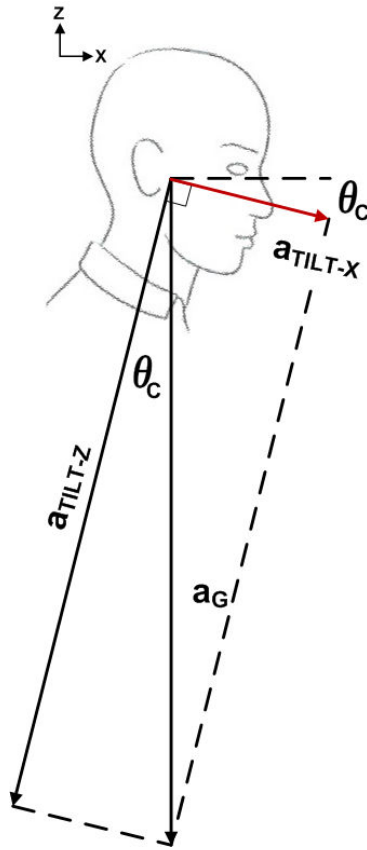


**Figure 17: Acceleration Vector of Tilt Sines**  
**Illustration adapted from Clément & Reschke (2008)**

Translation sines 49cm and 100cm are purely sinusoidal motions in translation with 49cm and 100cm in amplitude (i.e.  $D_c$ ) respectively. The linear displacement, velocity and acceleration with respect to time can be expressed by a set of simple harmonic motion equations (equations (3), (4), and (5)). The magnitude of maximum acceleration due to linear translation is expressed by equation (6). When linear acceleration vector and the gravity vector are summed, the resultant magnitude and angle are expressed by equations (7) and (8). Figure 18 illustrates the actual locations of the resultant vector relative to the human interaural axis.

$$x(t) = D_c \sin(\omega t) \quad (3)$$

$$v(t) = D_c \omega \cos(\omega t) \quad (4)$$

$$a(t) = -D_c \omega^2 \sin(\omega t) \quad (5)$$

$$a_{TRANS-X} = D_c \omega^2 \quad (6)$$

$$a_R = \sqrt{a_{TRANS-X}^2 + a_G^2} \quad (7)$$

$$\theta_R = \tan^{-1} \left( \frac{a_{TRANS-X}}{a_G} \right) \quad (8)$$

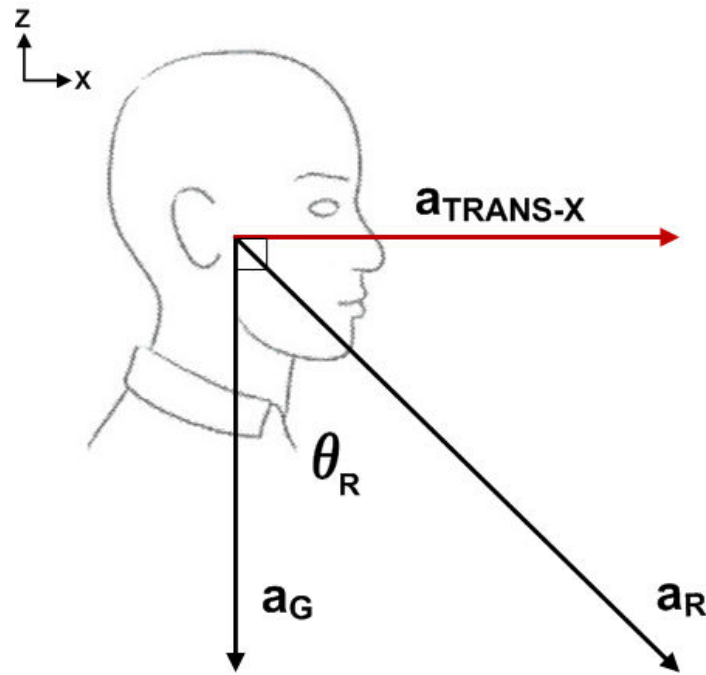


**Figure 18: Acceleration Vector of Translation Sines  
Illustration adapted from Clément & Reschke (2008)**

The Z-Axis Independent Gravitoinertial (ZIG) and Z-Axis Aligned Gravitoinertial (ZAG) motion profiles combine the two previous sinusoidal motion profiles such that tilt and translation have mutually constructive (i.e. in-phase) and destructive effects (i.e. out-of-phase), respectively. Figure 21 and Figure 22 illustrates the motion profiles of ZIG and ZAG, respectively. More specifically, during the ZIG sines motion profile, the subject is tilted forward and translated

forward allowing the constructive interference of the two motions to increase the angle of the resultant vector with respect to the subject's coordinate frame. Hence, the resultant vector is independent from the subject's longitudinal body axis (i.e. Z-axis). Figure 19 illustrates the acceleration vectors from tilt and translation motions acting the human vestibular organ in the ZIG motion profile. The resultant magnitude and angle from this motion profile are expressed by equations (9) through (12).

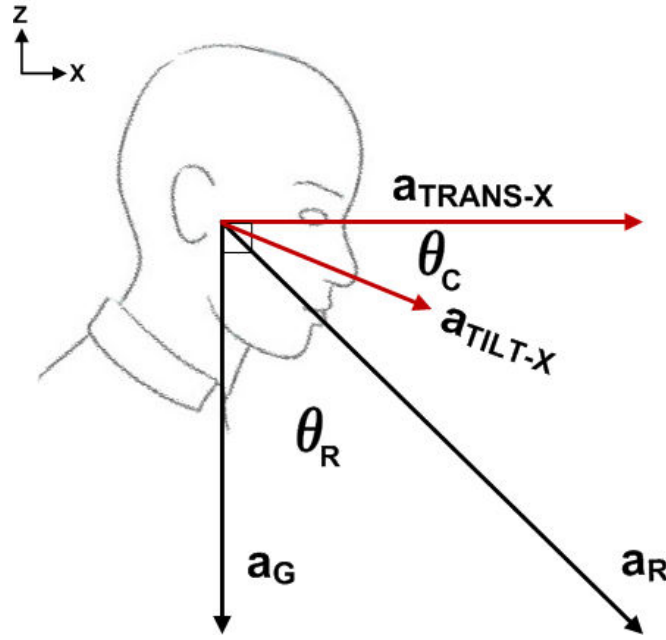


**Figure 19: Acceleration Vectors of ZIG Sines**  
**Illustration adapted from Clément & Reschke (2008)**

$$a_X = a_{TRANS-X} + a_{TILT-X} \cos \theta \quad (9)$$

$$a_Z = -a_G - a_{TILT-X} \sin \theta \quad (10)$$

$$a_R = \sqrt{a_X^2 + a_Z^2} \quad (11)$$

$$\theta_R = \tan^{-1} \left( \frac{a_X}{-a_Z} \right) \quad (12)$$

Conversely, during the ZAG sines motion profile, the subject is tilted backward and translated forward allowing the destructive interference of the two motions to align the resultant vector with the subject's longitudinal body axis. Figure 20 illustrates acceleration vectors from tilt and

translation motions acting the human vestibular organ in the ZAG motion profile. The resultant magnitude and angle from this motion profile are expressed by equations (13) and (14). Table 2 summarizes the actual magnitude and angle of the resultant acceleration vector for all of the motion profiles.

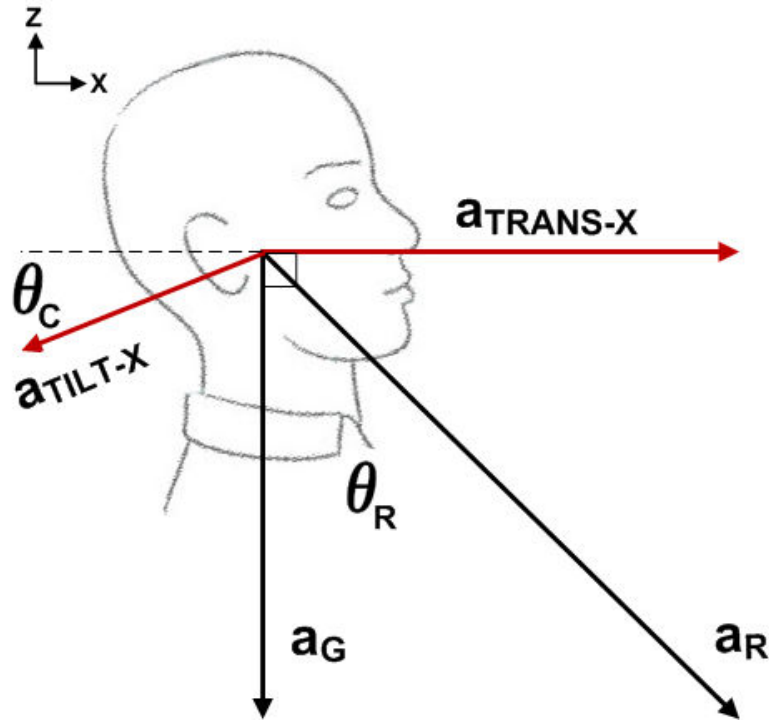


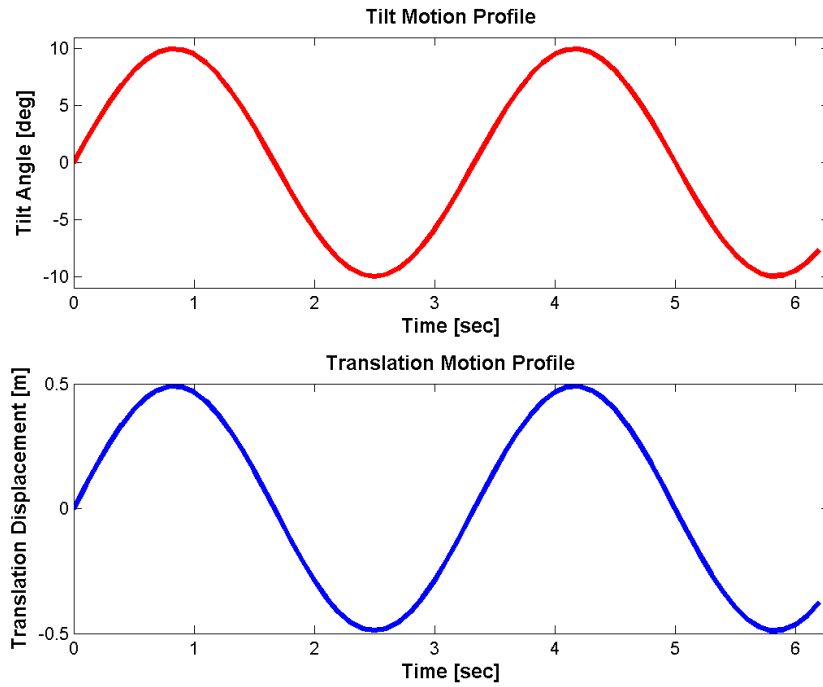
Figure 20: Acceleration Vectors of ZAG Sines  
Illustration adapted from Clément & Reschke (2008)

$$a_x = a_{TRANS-X} - a_{TILT-X} \cos \theta \quad (13)$$

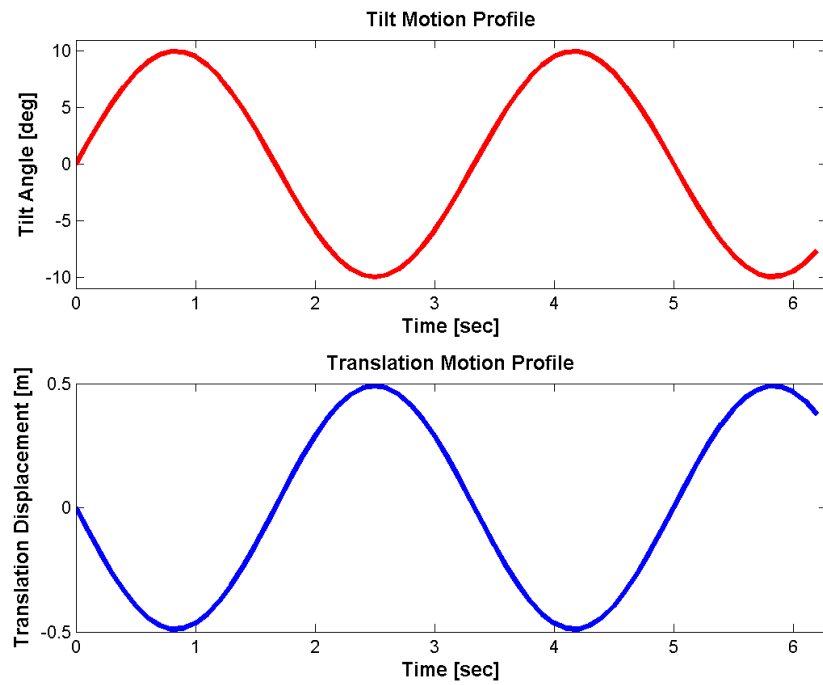
$$a_z = -a_G - a_{TILT-X} \sin \theta \quad (14)$$

Table 2: Summary of Actual Resultant Acceleration Parameters

	Max. Magnitude [g]	Max. Angle [deg]
Tilt Sines 10°	0.174	-10
Tilt Sines 20°	0.34	-20
Translation Sines 49cm	0.178	10
Translation Sines 100cm	0.36	20
ZIG Sines 10° 49cm	1.016	20
ZAG Sines 10° 49cm	0.95	0



**Figure 21: Z-Axis Independent Gravitoinertial (ZIG) Motion Profile**



**Figure 22: Z-Axis Aligned Gravitoinertial (ZAG) Motion Profile**

The frequency of 0.3Hz is used for all six of the motion profiles. As mentioned in the previous work (section 1.2), the frequency response of tilt and translation perception demonstrates clear evidence of segregation such that interpretation of tilt occurs mainly in the low frequency range and interpretations of translation occur mostly in the high frequency range. The cross over frequency of the two interpretations is somewhere between 0.3Hz to 0.4Hz. Hence, the intent of using 0.3Hz for all of the six profiles in this study is to obtain insight on how the CNS resolves perception of motion in a frequency that causes the most ambiguous cues.

## 2.5 Data Collection Methods

For each portion of the study, the subject was asked to provide verbal report on the perception of tilt or translation and to perform a manual task of actively replicating the perceived motion using a joystick. For the manual task, the subject was asked mimic the perceived amplitude and frequency of the motion. Specifically for the tilt perception, each subject was asked to report forward and backward angular displacements of the head. In addition, each subject was asked to estimate the location of the rotation axis relative to his/her head. As illustrated in Figure 23, one can perceive rotation axis to be in three locations, above the head, below the feet or somewhere in-between. The purpose of inquiring about this information is to determine the perceived relative phase of the two motions. For instance, if the subject perceives the rotation axis to be some distance above the head as illustrated in Figure 23A, then it is clear that the subject had perceived out-of-phase motion (i.e. ZAG): as the subject translates forward, the subject tilts backward. Conversely, if the subject perceives the rotation axis to be some distance below the head as illustrated in Figure 23B, then it is clear that the subject had perceived in-phase motion (i.e. ZIG): as the subject translates forward, the subject tilts forward as well. For translation perception, the verbal report is relatively simple: each subject was asked to report the peak-to-peak linear displacement.

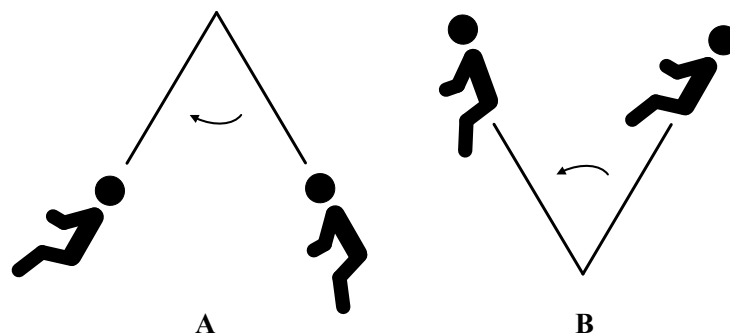


**Figure 23: Locations of Perceived Rotation Axis**

### **3 Considerations for Human Subject Testing**

Informed consent from each subject was obtained in accordance with institutional review board requirements. Each subject's participation is strictly voluntary and each subject may discontinue participation at any point without penalty and loss of benefits. Specifically, subjects were instructed about the risks of participation. The NASA Johnson Space Center Committee for the Protection of Human Subjects (CPHS) has rated this study to involve "reasonable" risks to the subject. NASA JSC CPHS defines this as follows:

"Reasonable risk" means that the probability and magnitude of harm or discomfort anticipated in the research are greater in and of themselves than those ordinarily encountered in daily life or during the performance of routine physical or psychological examinations or tests, but that the risks of harm or discomfort are considered to be acceptable when weighed against the anticipated benefits and the importance of the knowledge to be gained from the research (JSC FORM 1416, 2004).

A layman's summary of the experiment, which included the general purpose, experimental procedures and possible discomforts, was also given each subject. By signature, each subject understood that there was no direct personal benefit in participation but the study will help investigators better understand the resolution mechanisms of the human brain when presented with ambiguous motion cues. Financial compensation of civil servants (i.e. NASA employees) as test subjects is not permitted under United States Federal Law. Similarly, employees of WYLE, the prime contractor of Human Adaptation and Countermeasures Division, may not be compensated as test subjects. Subjects, who are employed by any other employer, are compensated USD\$10 per hour of participation.

Lastly, and also most importantly, each subject is informed of his/her rights of participation. According to the U.S. Privacy Act of 1974, each subject's medical history and generated data during experimentation will be kept confidential with appropriate means such as designated file system and coded identifiers. In the event of personal injury or personal property damage during experimentation, each subject has the right to claim reparation to the extent allowed by the Federal Employees Compensation Act or the Federal Tort Claims Act.

### 3.1 Risk and Hazards Analysis

Risk and hazards analysis is one of the critical elements of any life science research protocol, especially if the human subjects are involved. Potential threats to the life and wellbeing of the involved subjects and operators must be assessed and mitigated to provide adequate safeguard from personal discomfort, injury and property damage. The following analysis of potential hazards and associated risks is partially based on contents from existing research protocol involving the Tilt-Translation Sled (WOOD, S.J., 2009).

**Table 3: Severity and Likelihood Categories**

Severity		Likelihood	
1	Negligible	A	Improbable
2	Moderate	B	Extremely Low
3	Critical	C	Low
4	Catastrophic	D	Medium
		E	High

Severity	4		#2, #5	#4		
	3		#1	#6		
	2		#3	#8	#7	
	1					
		A	B	C	D	E
		Likelihood				

**Figure 24: Pre Risk Mitigation Assessment**

Severity	4					
	3	#1, #5	#2, #4			
	2	#3	#6, #8			
	1			#7		
		A	B	C	D	E
		Likelihood				

**Figure 25: Post Risk Mitigation Assessment**

**Potential hazard #1:** Uncontrolled seat rotation and/or end-of-travel (EOT) limit in translation

Causes – Error in command input and/or failure in servo feedback control loop

Effects - Uncontrolled machine behavior causing subject/operator injury

Pre-risk mitigation assessment - Severity = Critical; Probability = Extremely Low

Methods to minimize risks –

- Software limits for position, velocity and acceleration for both tilt and translation axes have been implemented. Additionally, all servo drives continuously monitor for loss of encoder feedback and excessive command input.

- Hardware end-of-travel limits have been implemented using two pneumatic pistons to provide deceleration with no more than 2g in worst case scenarios.
- Test profiles are examined prior to subject ingress.
- Procedural check points have been implemented such that motion will begin only after subject is secured and all operators are cleared from the operating space. Additionally, start-up procedures include verification for home tilt and home translation positions.
- Redundant emergency stop buttons on the control console are available and easily accessible to all operators.

Post-risk mitigation assessment - Severity = Critical; Probability = Improbable

**Potential hazard #2: Structural Failure**

Cause - Impact from unsecured objects, impact with rotator, components failure

Effects - Death or personal Injury

Pre-risk mitigation assessment - Severity = Catastrophic; Probability = Extremely Low

Methods to minimize risks –

- All safety critical fasteners will be fitted with lock washers or lockwire. Loctite 262 will be used on all critical fasteners.
- The safety factor of 1.5 will be validated by proof load test using maximum operational load and using approximately 95% percentile male subject.
- Procedurally, the operator will clear the operating space of TTS before engaging any actuators. The emergency stop button will be used if any object or person passes beyond the secured boundary.
- The subject will be secured in the seat with a five-point harness and will be monitoring by the operators with infrared video surveillance.

Post-risk mitigation assessment - Severity = Critical; Probability = Extremely Low

**Potential hazard #3: Subject neck or back injury**

Cause - Uncomfortable positioning due to subject restraint components

Effects - Personal Injury

Pre-risk mitigation assessment - Severity = Moderate; Probability = Extremely Low

Methods to minimize risks –

- Subject's head and neck are restrained by moldable pads and adjustable supports to ensure appropriate fit.
- During the motion profiles, operators continuously remind subjects to not make drastic movements and maintain an upright position of the head and neck.
- Continuous audio communication and video surveillance will ensure that subject will be able to voluntarily stop the experiment upon any discomfort or pain.

Post-risk mitigation assessment - Severity = Moderate; Probability = Improbable

**Potential hazard #4:** Subject unable to perform emergency egress

Cause - Emergency egress required with disorientation and/or motion sickness symptoms

Effects - Death / Personal Injury

Assessment - Severity = Catastrophic; Probability = Low

Methods to minimize risks –

- Subjects will be briefed on reporting nausea sensations on a scale of 0-10, with 10 being extremely nauseous. The operator will continuously ask for comfort and nausea levels. Tests will be terminated with nausea levels exceeding 4 out of 10.
- Egress will be facilitated by the use of quick release restraint fasteners, allowing the subject to release restraints independently if necessary.
- Operators will assist the subject in the event of a facility emergency that requires rapid egress from TTS. In the event of a facility power loss, the motion will come to a complete stop within 1 min with the chair in the unloading position.

Post-risk mitigation assessment - Severity = Critical; Probability = Extremely Low

**Potential hazard #5:** Subject/operator electrical shock

Cause - Improperly grounded instrumentation, cable binding, failure of electrical insulation

Effects - Death / Personal Injury

Assessment - Severity = Catastrophic; Probability = Extremely Low

Methods to minimize risks –

- All power cables will be suitably insulated and proper strain-relief will be used to avoid mechanical stress on electrical wires in static and during motion.
- Annual electrical continuity inspection will be performed to avoid improper grounding.
- Procedurally, operators are tasked to visually inspect all power and data cables in proximity of the subject prior to experimental session.
- All electrical work meets or exceeds the requirements of National Fire and Protection Association (NFPA) National Electric Code (NFPA 70). Standard lock-out/tag-out procedures will be implemented for electrical power subsystems maintenance.

Post-risk mitigation assessment - Severity = Critical; Probability = Improbable

**Potential hazard #6:** Subject eye injury

Cause - Exposure to near-infrared radiation from camera mounted inside the TTS enclosure or from the head-mounted binocular camera system

Effects - Personal Injury

Assessment - Severity = Critical; Probability = Low

Methods to minimize risks –

- Near-infrared emitting diodes (IREDs) will be used to illuminate the eyes under dark conditions. The intensity and cumulative duration of exposure will be within the boundaries set by the American Conference of Governmental Industrial Hygienists (ACGIH).
- Dichroic or split beam type mirrors will be attached to the head-mounted camera system in order to provide full binocular field of view for eye tracking. The mirrors are securely

mounted such that possible displacements of the mirrors are limited by mechanical means.

Post-risk mitigation assessment - Severity = Moderate; Probability = Extremely Low

**Potential hazard #7: Motion Sickness**

Cause - Experiencing a complex and/or ambiguous motion stimuli

Effects - Personal Discomfort

Assessment - Severity = Moderate; Probability = Medium

Methods to minimize risks –

- Experimental sessions are limited to less than 1 hour in duration.
- Operators continuously monitor and communicate with the subject to ensure subject is comfortable. Each subject is reminded of reporting any symptoms of nausea. The session will immediately stop when the subject reports onset of motion sickness symptoms such as excessive sweating and swallowing as well as heavy breathing. A nausea scale of 0 to 10 will be used as a quantitative reference for onset of motion sickness. Reports of 4 or 5, will warrant termination of the session.

Post-risk mitigation assessment - Severity = Negligible; Probability = Low

**Potential hazard #8: Slipping, tripping, falling**

Cause – Obstacles during ingress and/or egress, unsecured wires or other equipment, cluttered operating environment

Effects - Personal Injury

Assessment - Severity = Moderate; Probability = Low

Methods to minimize risks –

- Operators are tasked to assist during ingress and/or egress.
- Procedurally, operators are tasked to clear the operating environment free of clutter prior to the start of each experimental session. General good housekeeping practices in the laboratory will be maintained.
- All potential obstacles are labeled clearly with caution tape.

Post-risk mitigation assessment - Severity = Moderate; Probability = Extremely Low

## 4 Results

The results presented here derive from data collected from 11 out of the total 12 subjects tested. One subject's data was omitted in the analysis due to excessive sensations of nausea. As described in section 2.2 (methods), the operator stops the motion profile as soon as the subject reports the nausea level to be greater than or equal to 4 out of a 0-10 nausea scale. Subsequently, the reported perception values from this subject are compared with those from other subjects and these values are evidently outliers in the data set. Error bars in the following plots of mean values indicate standard error of mean (SEM)

### 4.1 Tilt and Translation Calibrations

As described in the experimental procedures (section 2.3), each subject is trained and calibrated to various tilt and translation displacements. The calibration data for each subject is plotted and a best-fit linear regression is determined. The gain (i.e. slope of the linear regression) value quantifies the subject's perception with respect to actual displacements. This technique allows comparison amongst all subjects. For example, Figure 26 and Figure 27 are calibration plots for subject number 2.

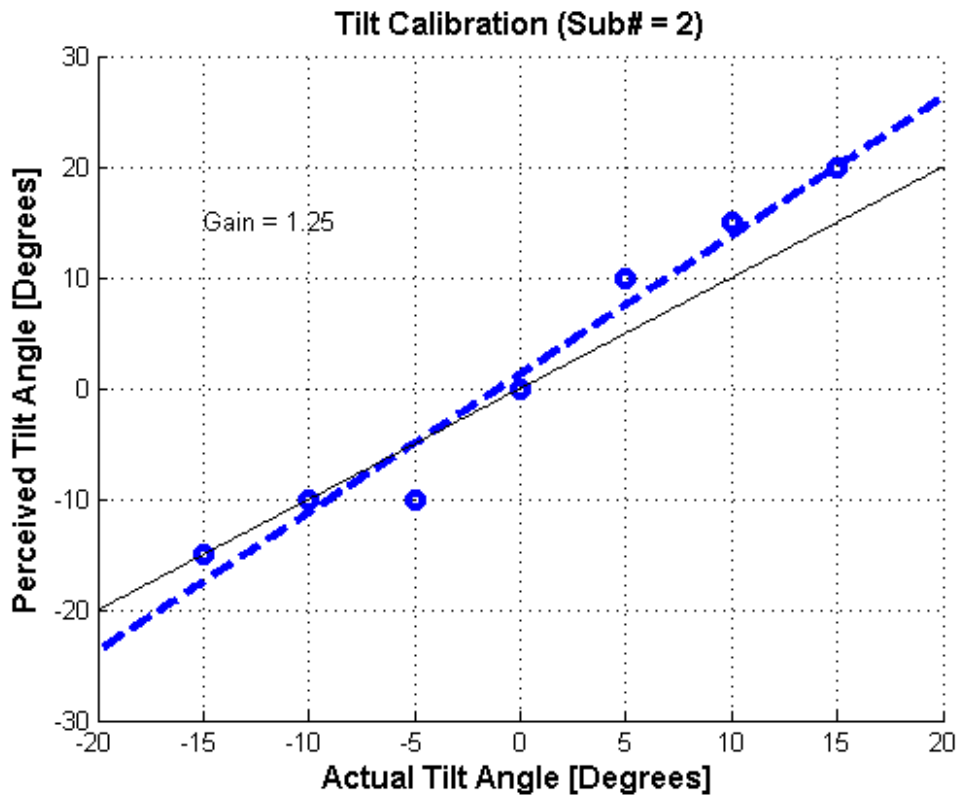


Figure 26: Tilt Perception Calibration

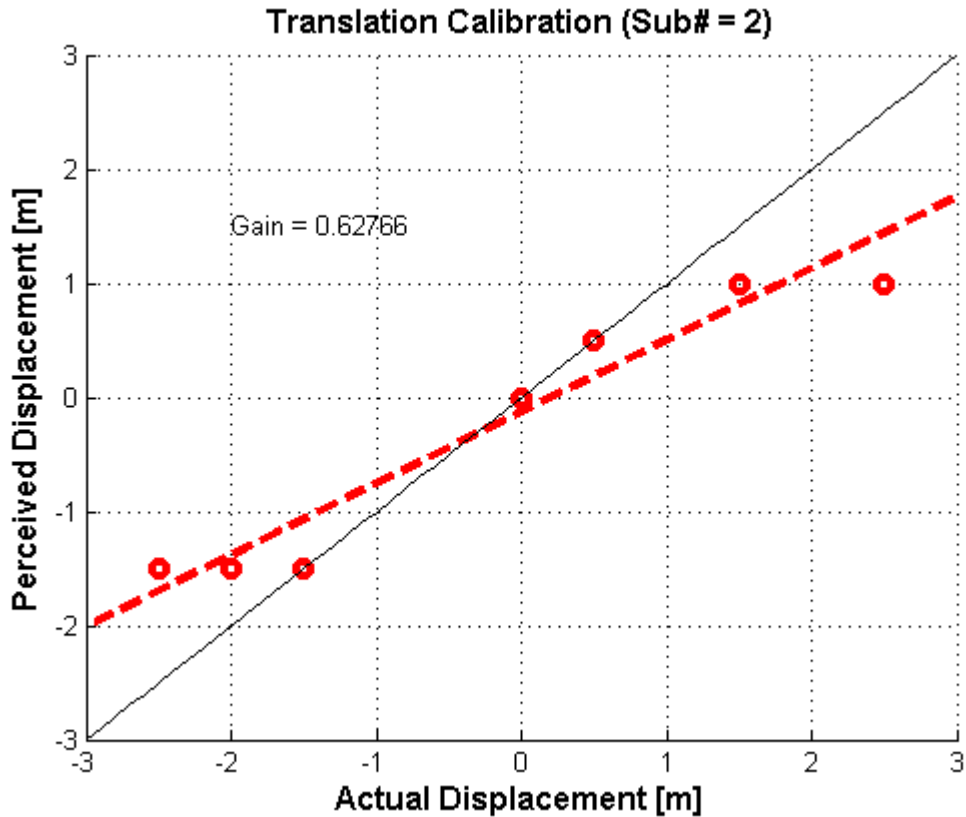
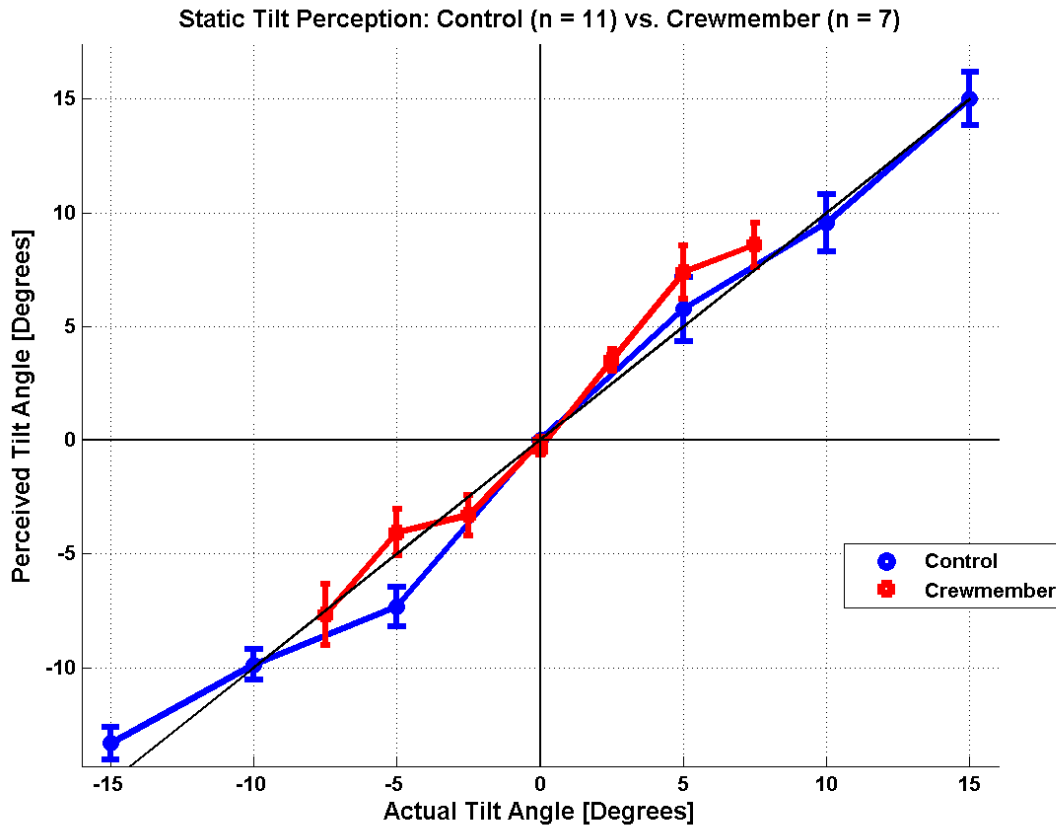


Figure 27: Translation Perception Calibration

#### 4.2 Effects of Training in Tilt

Since one of the novel features of this study is training the subject on perceiving incremental tilt and translation displacements, it is prudent to examine its effectiveness. As a method of benchmarking, the collective tilt calibration results from all subjects in this study are compared with the results collected from crewmembers of the ongoing ZAG study. From Figure 28, it is evident that after training, subjects from the general public with no extensive pilot background performed similarly in tilt as crewmembers. Hence, the brief training in tilt proves to be quite effective in the range of  $\pm 15$  degrees. Subjects generally do well in estimating the actual tilt because each angular displacement is evaluated against the vertical reference with which most people are familiar, even without visual cues.



**Figure 28: Static Tilt Perception: Control vs. Crewmembers**

### 4.3 Effects of Training in Translation

Similar to the analysis of tilt training, the average results from translation training is plotted in Figure 29. Evidently, subjects generally underestimate linear displacement and the deviation from actual linear displacement is quite significant. This may have implication on the design of next generation visual display onboard man-rated spacecrafts. Since the lack of visual cues hinders the accurate estimation of translation, it would be favorable for human operators to receive some reference signals that is either visual or tactile in nature.

The trend demonstrates that as the distance increases, the human perception of translation would possibly have two behaviors: one, perception for both forward and backward saturates to some constant value; two, both perception increases and decreases after some threshold distance. This could be the translation equivalent of the Aubert – Müller effect (i.e. A-E effect), where perception of tilt actually decreases as the actual tilt angle increases (HOWARD, I.P., 1982). Figure 30 illustrates this phenomenon.

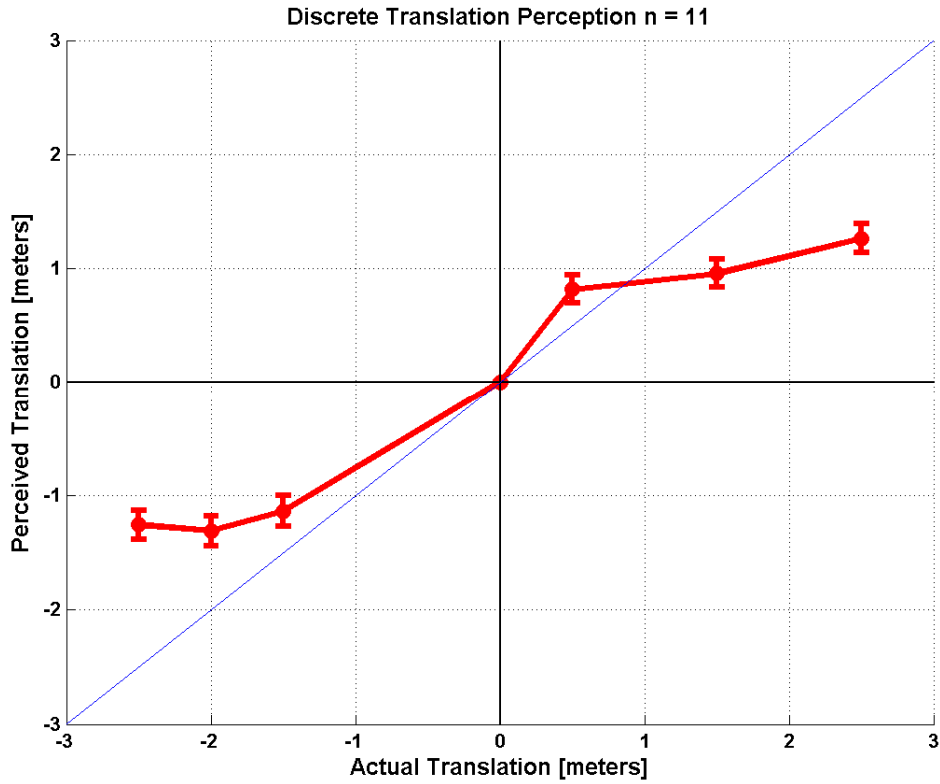


**Figure 29: Static Translation Perception**

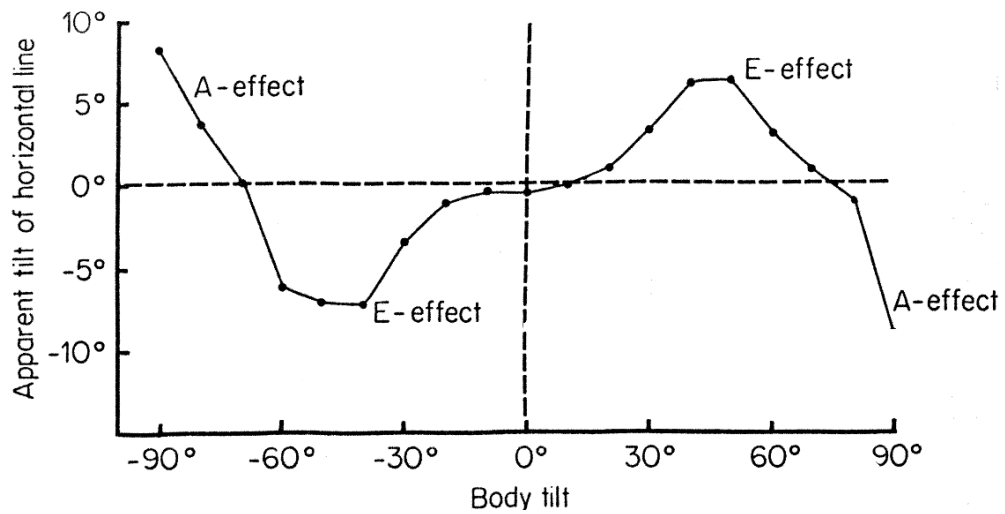


**Figure 30: The Aubert – Müller Effect**  
Figure courtesy of Howard (1982)

#### 4.4 Dynamic Tilt Perception

During the six sinusoidal motion profiles, each subject was asked to focus purely on his/her perception of tilt. Figure 31 plots the perceptual verbal reports in forward tilt (i.e. positive degrees) and backward tilt (i.e. negative degrees). For pure tilt motions (i.e. Tilt Sines 10d and 20d), subjects can perceive the relative change in amplitude but they cannot perceive the correct actual angular displacements. For pure translation motions (i.e. Trans Sines 49cm and 100cm), the general perceptions are correct in that sensations of tilt are minimal. This is consistent with the fact that the semi-circular canals are not activated in the pure translation (i.e. no evidence of hill top illusion). When comparing the tilt perceptions of ZIG and ZAG motion profiles, it is evident that the tilt sensation for ZIG is relatively higher than that of ZAG. However, when compared with control (i.e. Tilt Sines 10°), the SEM of ZIG tilt perception overlaps that of Tilt Sines 10°, and the mean value is lower than 20°, which is the actual angle of the resultant vector. This result is not consistent with part one of the hypothesis, which expects an increase in tilt perception for ZIG compared to control. The tilt perception of ZAG can be attributed to activated semi-circular canals in the 0.3Hz stimulus frequency. In other words, although the resultant GIF vector is aligned with the longitudinal body axis of each subject, the sense of rotation at the head is detected by the canals. Overall, the backward tilt perception is lower than forward tilt perception. This asymmetry in estimating angular displacement is perhaps due to habituation of the subject sitting in a chair with a five-point harness. Since the somatosensory receptors of the posterior have been saturated in seated position, the anterior receptors are thus relatively more sensitive. An alternative interpretation for the asymmetry between backward and forward tilt comes from the physiology of the ankle joint. The human ankle joint physically allows larger amplitude in forward motion than backward motion. In daily activities, humans generally tilt body forward and step backward to control equilibrium posture. Hence, the brain is preconditioned to be more sensitive in evaluating forward tilt than backwards tilt perceptions.

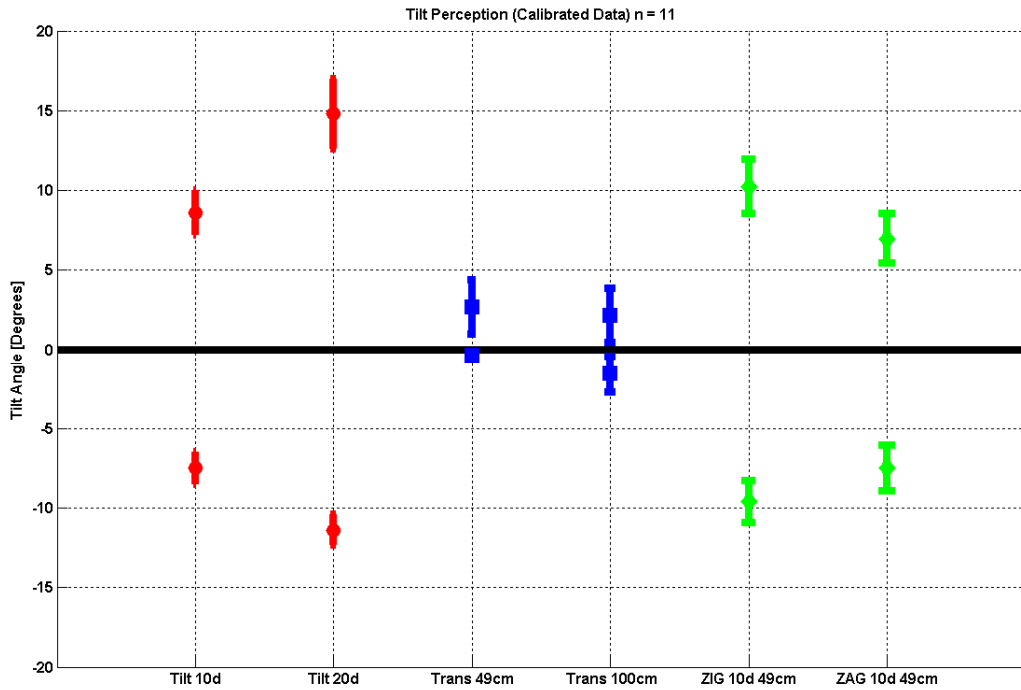


**Figure 31: Dynamic Tilt Perception**

#### 4.5 Dynamic Translation Perception

For the same six motion profiles, the subjects were asked to focus only on translation of the head and disregard any sensations of tilt. In the verbal report, each subject estimated the approximate peak-to-peak linear displacement that he/she perceived. Figure 32 plots the amplitude, i.e. half of the peak-to-peak translation perception. For motion profiles with pure tilt, there is no statistical significance since the SEM overlap between the two motions. For motion profiles with pure translation, the general perception is overestimation. This phenomenon can be attributed to a shift of crossover frequency between motion paradigms. Although previous work clearly indicates that the crossover frequency is between 0.3 and 0.4Hz, this result might be specific to rotations about the z-axis. Since this study stimulates the subjects in the fore-aft direction and in the pitch plane only, the crossover frequency is perhaps lower than 0.3Hz, which explains the overestimation of translation perception. Finally, there is no statistical significance between ZIG and ZAG results, nor is there clear increase in sense of translation in ZAG compared with the control profile (i.e. Trans Sines 49).

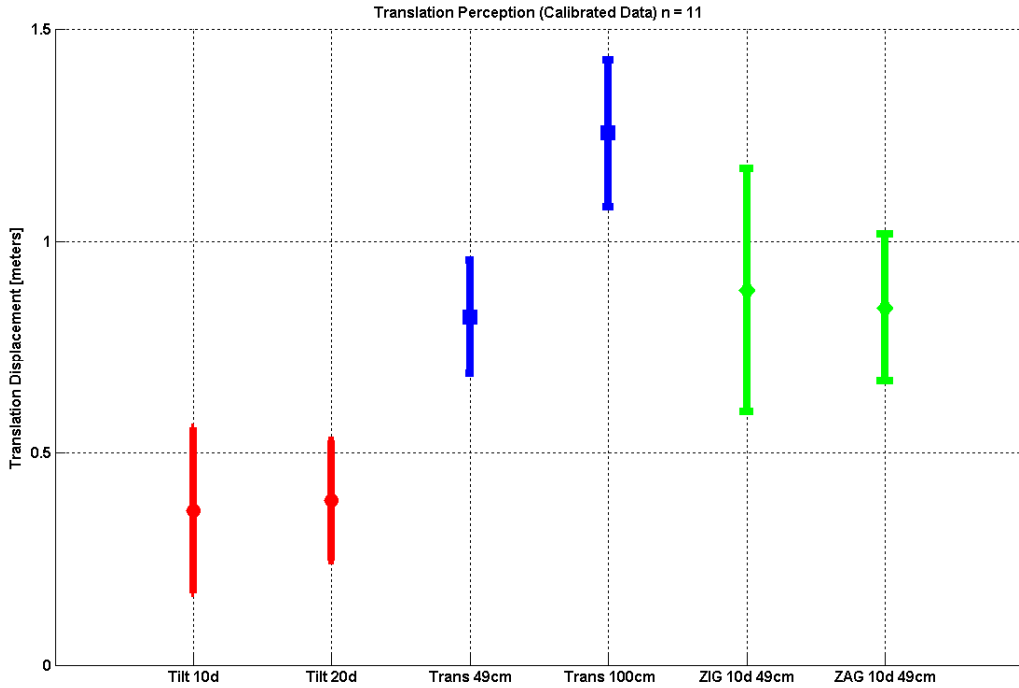


**Figure 32: Dynamic Translation Perception**

#### 4.6 Axis of Rotation Locations

While the subjects are asked to focus solely on the tilt perception, each one was asked to estimate the location of the rotation axis relative to the head for every motion profile. If the brain can correctly decouple the angular and linear components of the actual motion, then the perceived angles of tilt  $\theta_p$  and perceived distances of translation  $X_p$  would be consistent with the perceived location of the rotation axis  $Z_p$  through simple trigonometry. The location of the perceived rotation axis can be calculated according to the following expression:

$$Z_p = \frac{X_p}{\tan \theta_p} \quad (15)$$

The sign of  $Z_p$  must be determined from subject verbal report indicating above or below the head. If the subject reports the axis to be located at the head (i.e. the interaural axis), then his/her data is omitted for this particular analysis. Figure 34 plots the absolute difference between the calculated and the report locations of the rotation axis; hence, low errors indicate consistent estimation. It is no surprise that the subjects are collectively more consistent for tilt than for translation. This observation is also true for ZIG versus ZAG. Since tilt perception is quite prevalent in ZIG profiles, the subjects can decoupling tilt and translational component more

accurately than in ZAG profiles. Another explanation for relatively large estimation errors for ZAG is that while the otolith stimuli is minimized by the alignment of resultant vector to the subject z-axis, the canals are still activated at 0.3Hz. This isolation in stimulation perhaps leads to enough interaural conflict to hinder the CNS in decoupling ambiguous inertial motion cues.

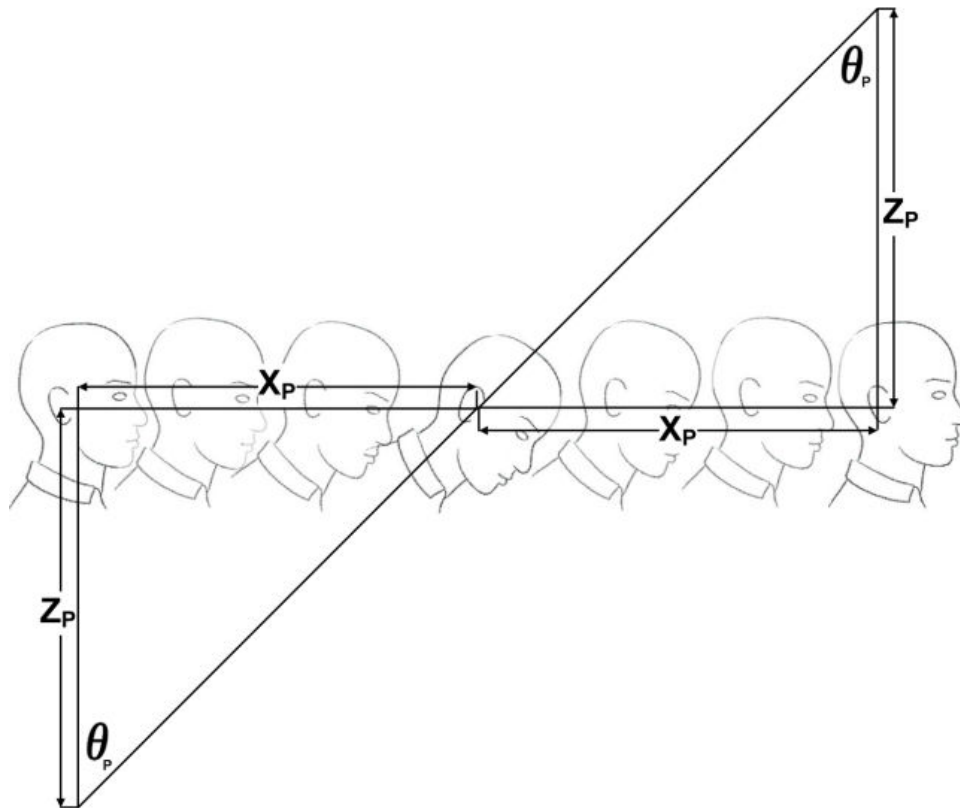


**Figure 33: Rotation Axis Locations**  
Illustration adapted from Clément & Reschke (2008)

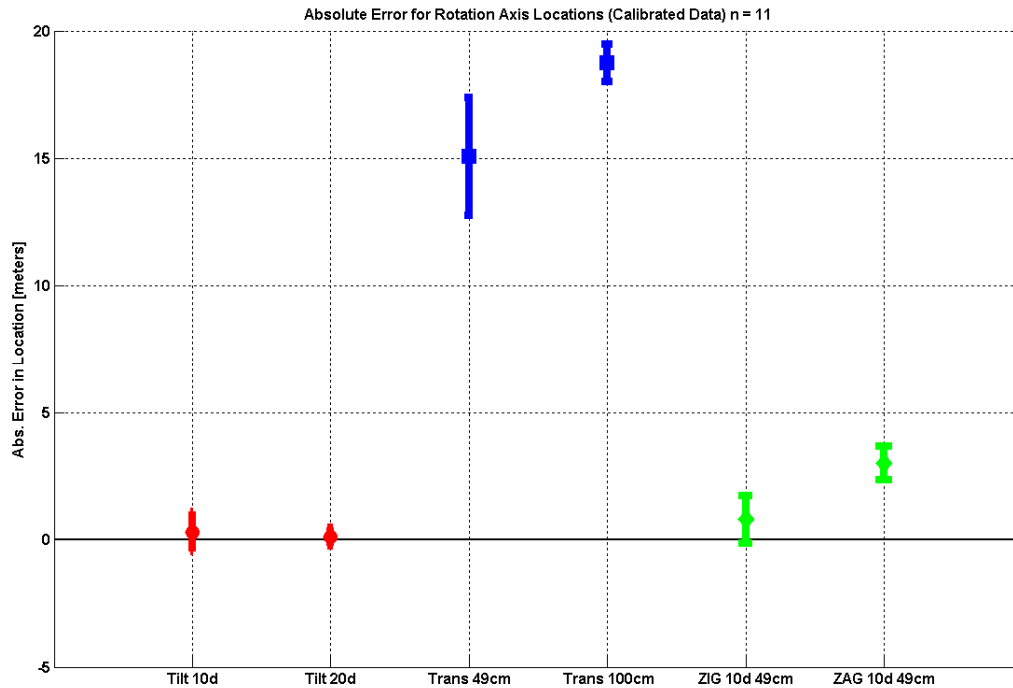


**Figure 34: Absolute Difference in Rotation Axis Locations**

#### 4.7 Resultant Acceleration Analysis

In section 2.4, the actual acceleration values are calculated for each of the six motion profiles. With perceptual verbal reports, it is possible to calculate the perceived acceleration values and compare the resultant acceleration magnitude and angle. As described previously in section 2.5, the location of rotation axis relative to the interaural axis can indicate either in-phase (i.e. ZIG) or out-of-phase motion (ZAG). Additionally, when the rotation axis is not located at the interaural axis, the subject essentially perceives motion similar to either a normal pendulum or an inverted pendulum. Through fundamental mechanics, all parameters of the verbal report can be used to calculate the magnitude and angle of the resultant acceleration vector.

The simple harmonic motion of a pendulum can be summarized by equations (16) to (18). The tangential maximum acceleration for a point mass with weightless bar can be expressed by equation (19). The acceleration vectors based on perceptions of tilt and translation are illustrated in Figure 35 for rotation axis above the head and in Figure 36 for rotation axis below the head.

$$\theta(t) = \theta_P \sin(\omega t) \quad (16)$$

$$\dot{\theta}(t) = \theta_P \omega \cos(\omega t) \quad (17)$$

$$\ddot{\theta}(t) = -\theta_P \omega^2 \sin(\omega t) \quad (18)$$

$$a_{POINT} = -D_{AXIS} \cdot \theta_P \omega^2 \quad (19)$$

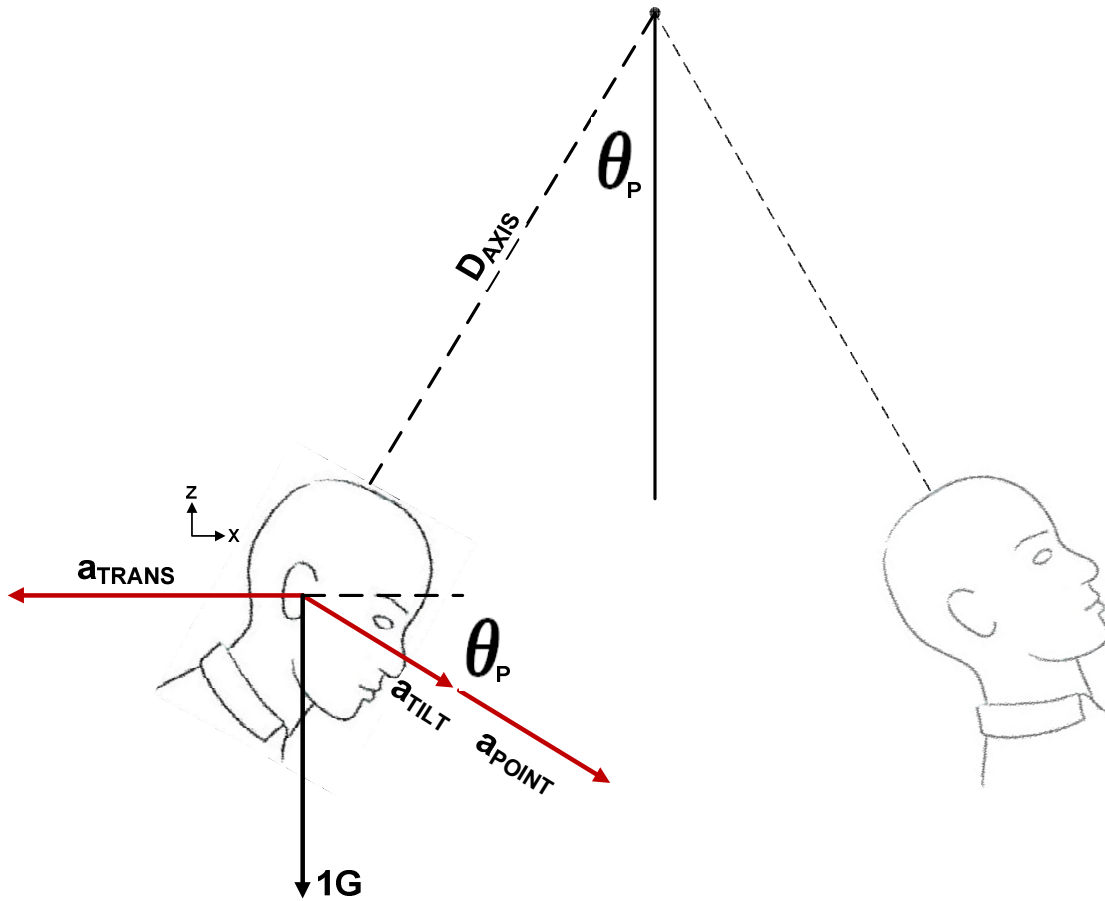


**Figure 35: Perceived Accelerations When Rotation Axis is Above the Head  
Illustration adapted from Clément & Reschke (2008)**

For reports of rotation axis above the head, the components of acceleration in the  $x$  and  $z$  directions can be expressed by equations (20) and (21). Alternatively, for reports of rotation axis below the head, the components of acceleration in the  $x$  and  $z$  directions can be expressed by equations (22) and (23).  $D_{TRANSP}$  is the perceived amplitude of translation and  $D_{AXIS}$  is the

perceived location of rotation axis relative to the head. The resultant magnitude and angle can be expressed by equations (24) and (25).

$$a_X = (a_{TILT} + a_{POINT}) \cos \theta_P - D_{TRANSP} \cdot \frac{\omega^2}{a}$$

$$a_X = \left( a_G \sin \theta_P + \frac{D_{AXIS} \cdot \theta_P \omega^2}{a} \right) \cos \theta_P - D_{TRANSP} \cdot \frac{\omega^2}{a} \quad (20)$$

$$a_Z = -a_G - (a_{TILT} + a_{POINT}) \sin \theta_P$$

$$a_Z = -a_G - \left( a_G \sin \theta_P + \frac{D_{AXIS} \cdot \theta_P \omega^2}{a} \right) \sin \theta_P \quad (21)$$

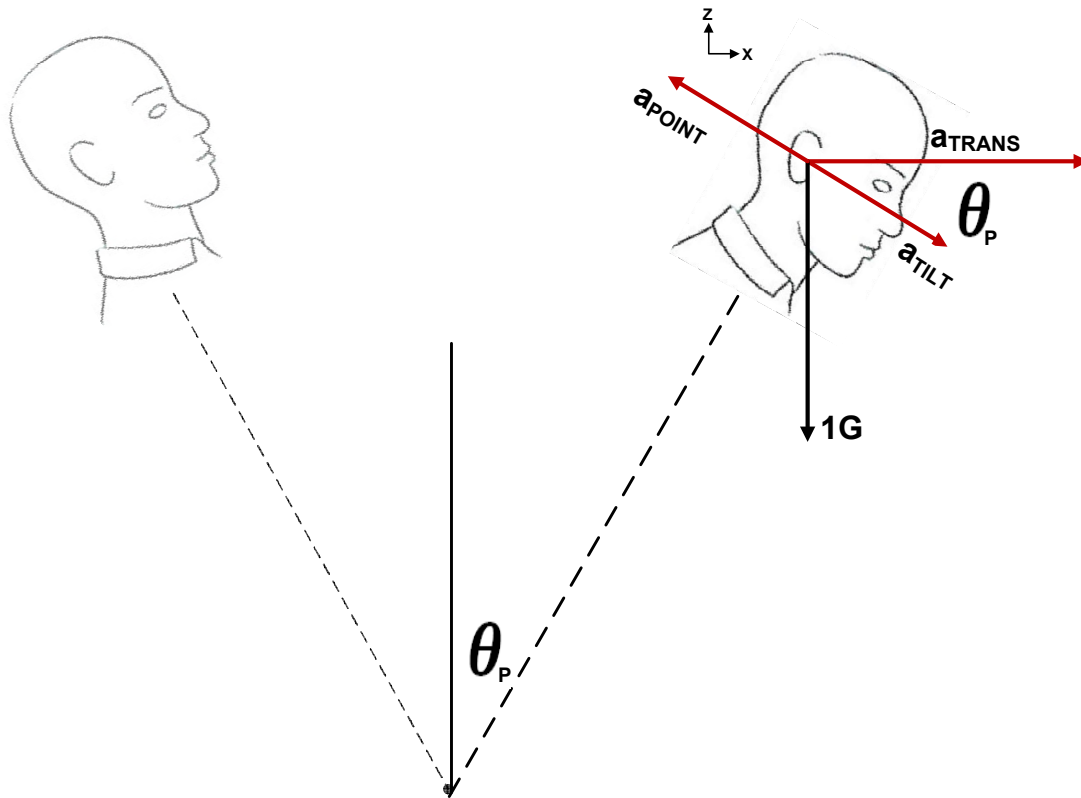


**Figure 36: Perceived Accelerations When Rotation Axis is Below the Head**  
Illustration adapted from Clément & Reschke (2008)

$$a_X = (a_{TILT} - a_{POINT}) \cos \theta_P + D_{TRANSP} \cdot \frac{\omega^2}{a}$$

$$a_X = \left( a_G \sin \theta_P - \frac{D_{AXIS} \cdot \theta_P \omega^2}{a} \right) \cos \theta_P + D_{TRANSP} \cdot \frac{\omega^2}{a} \quad (22)$$

$$a_Z = -a_G - (a_{TILT} - a_{POINT}) \sin \theta_P$$

$$a_Z = -a_G - \left( a_G \sin \theta_P - \frac{D_{AXIS} \cdot \theta_P \omega^2}{a} \right) \sin \theta_P \quad (23)$$

$$a_R = \sqrt{a_x^2 + a_z^2} \quad (24)$$

$$\theta_R = \tan^{-1} \left( \frac{a_x}{a_z} \right) \quad (25)$$

Gain values for each of the motion profiles can be evaluated by the ratio of perceived acceleration parameters to actual acceleration parameters. The gains for magnitude and angle are plotted in Figure 37. For subjects who report that the axis of rotation is located at the interaural axis, the phase relationship between tilt and translation is indeterminate. Therefore, this particular subject's data cannot be useful for this analysis. The n values along the x-axis indicate the subject population size. For tilt only motion profiles, it is evident that the relevant subjects all tend to overestimate the magnitude and the angles of the resultant acceleration vector. The SEM of the two profiles overlaps such that there is no statistical difference between the two results. For translation only motion profiles, the estimates of magnitude correspond almost exactly to the actual resultant vector. Yet, the perceived resultant angles for both translation profiles are underestimates from the actual angles. For ZIG and ZAG, the results are equally nebulous. Although both ZIG and ZAG results show overestimation in magnitude, the large variations in angle gain makes any distinct observations inconclusive.

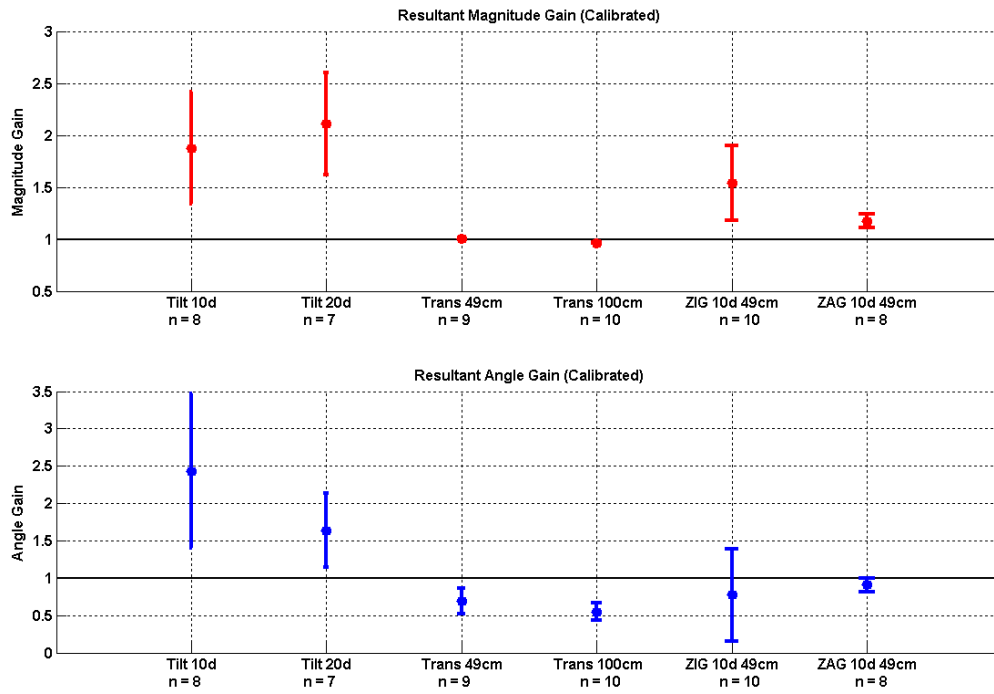


**Figure 37: Resultant Acceleration Analysis**

## 5 Discussion

The human perceptions of ambiguous tilt and translation motions in the frequency 0.3Hz have been characterized using the Tilt-Translation Sled at the Neuroscience Laboratory of NASA Johnson Space Center. The purpose of this study was to gather insight of the human neural mechanism for effective distinction between tilt and translational inertial motion cues. Specifically, this study used the GIF resolution hypothesis by Merfeld as the theoretical framework.

By using two unique motion paradigms to elicit either enhanced tilt perception (i.e. ZIG) or enhanced translation perception (i.e. ZAG) compared to respective control paradigms, this study aimed to validate the neural capacity to decouple ambiguous inertial motion cues such that when the perception of one component increased the perception of other component decreased, vice versa. Preliminary analysis of perceptual data did not indicate that the GIF resolution hypothesis is completely valid for non-rotational periodic motions.

The attributing reason could be the disparity in motion paradigms and method of capturing human perception. The seminal work on developing the GIF resolution principle rotated human subjects vertically about the Earth vertical axis and then tilted the same subjects by 90° about the interaural axis. As the subjects are oriented to discrete tilt positions about the body z-axis, binocular eye movements were recorded (MERFELD, D. et al., 1999). The purpose of rotation about the body z-axis prior to tilt is a method of saturating the semi-circular in order to reduce interaural conflict when examining responses of the otolith. VOR was induced and tracked at each orientation increment. The experimental setup of this study is inherently different in that the directions of stimuli are along the body x-axis (i.e. fore-aft) and about the body pitch plane. Since there were no rotations of the canals about the y-axis prior to the motion profiles and that all profiles operated at the frequency of sensitive canal response (i.e. 0.3Hz), the subjects must have experienced afferent signals from both the canals and the otolith organs. The resulting interaural conflict might have contributed to the high variability of verbal reports, making it difficult to identify observable perceptual differences.

Future work of this research effort includes analysis of subject's real-time perception data captured by the joystick. Additionally, critical tracking and hovering manual control tasks will be implemented with the visual feedback of onscreen displays. The objective is to evaluate the motor response to multisensory afferent signals in order to establish a relationship between vestibular misperceptions to control errors.

## 6 Works Cited

- ANGELAKI, D. E., M.Q. MCHENRY, D. DICKMAN et al. 1999. Computation of Inertial Motion: Neural Strategies to Resolve Ambiguous Otolith Information. *Journal of Neuroscience*. 19(1), pp.316-327.
- BENSON, A.J. 1982. The Vestibular Sensory System. *In: H.B. BARLOW and J.D. MOLLON, (eds). The Senses*, New York: Press Syndicate of the University of Cambridge, pp.333-368.
- CLÉMENT, G. 2005. *Fundamentals of Space Medicine*. Dordrecht: Springer.
- CLÉMENT, G. and D. HAMILTON. 2003. *Fundamentals of Space Medicine*. [online].
- CLÉMENT, G. and M. F. RESCHKE. 2008. *Neuroscience in Space*. New York: Springer.
- HOWARD, I.P. 1982. Visual Orientation to Gravity. *In: Human Visual Orientation*, Toronto: John Wiley & Sons Ltd, pp.412-442.
- JSC FORM 1416. 2004. *NASA JSC Human Subject Informed Consent*. Houston: NASA.
- MERFELD, D., L. ZUPAN, and R.J. PETERKA. 1999. Humans use internal models to estimate gravity and linear acceleration. *Nature*. 398, pp.615 - 618.
- PALOSKI, W.H., C.M. OMAN, J.J. BLOOMBERG et al. 2008. Risk of Sensory-Motor Performance Failures Affecting Vehicle Control During Space Missions: A Review Of The Evidence. *Journal of Gravitational Physiology*. 15(2), pp.1-29.
- WOOD, S.J. 2004. *NASA JSC Human Research Informed Consent*. Houston: NASA JSC.
- WOOD, S.J. 2009. *NASA JSC Life Science Research Protocol*. Houston.

## Appendix

Subject ID: \_\_\_\_\_ Session: \_\_\_\_\_ Date: \_\_\_\_\_

	Med Monitor:	Phone:	Operators:
Pre-Test	<input type="checkbox"/> Log book, clear operating envelopes, clean track, & power up console and ancillary equipment <input type="checkbox"/> Air on (90psi), audio & video surveillance, preset chair height, clean head restraint Power up control computer (user: Administrator, PW: neuroIRT), and main power to sled Launch Control client and verify profiles, center track, enable drives and run test profile Enter filename: ID-ZZ-, Load DVR, Prepare device for subject loading, prepare worksheets Complete pre-test questionnaire, protocol, motion sickness and emergency procedure briefing		
	Don harness, adjust chair height, don headphones and COM check Position MS bag, verify door latch closed and center box on track, verify personnel ready Start DVD recording, Set Max Recording Time		
Subj Load	<b>Tilt Training Run (0, -10°, -15°, -20°, 0°, +10°, +15°, +20°)</b>		
	<b>Tilt Calibration (TILTstep)</b>		
Test-Operations	Pre 0°:	3. Back 15°:	6. Forward 15°:
	1. Back 5°:	4. Forward 5°:	Post 0°:
	2. Forward 10°:	5. Back 10°:	
	<b>Condition Order 1</b>	<b>Angles</b>	<b>Axis of Rotation</b>
	TILTsin-f30-10d0cm		
	TILTsin-f30-20d0cm		
	TRANSsin-f30-0d49cm		
	TRANSsin-f30-0d100cm		
	ZIGsin-f30-10-49cm		
	ZAGsin-f30-0d49cm		
Tilt Perception	TILTsin		
	TRANSsin		
	ZIGsin		
	ZAGsin		
	<b>Translation Training Run (0, -0.5m, -1.0m, -1.5m, +0.5m, +1.0m, +1.5m)</b>		
	<b>Translation Calibration (TRANSstep)</b>		
	Pre 0m:	3. Forward 1.5m:	6. Back 1.5m:
	1. Forward 0.5m:	4. Back 0.5m:	Post 0m:
	2. Back 1.0m:	5. Forward 1.0m:	
	<b>Peak to Peak</b>		
TILTsin-f30-10d0cm			
TILTsin-f30-20d0cm			
TRANSsin-f30-0d49cm			
TRANSsin-f30-0d100cm			
ZIGsin-f30-10-49cm			
ZAGsin-f30-0d49cm			
TILTsin			
TRANSsin			
ZIGsin			
ZAGsin			
Post	Return enclosure to load position and disable drives, assist subject egress, complete debrief		
	Stop DVR recording, copy files to folder (ID-TTS-Session-DDMMYY) & backup, log test		

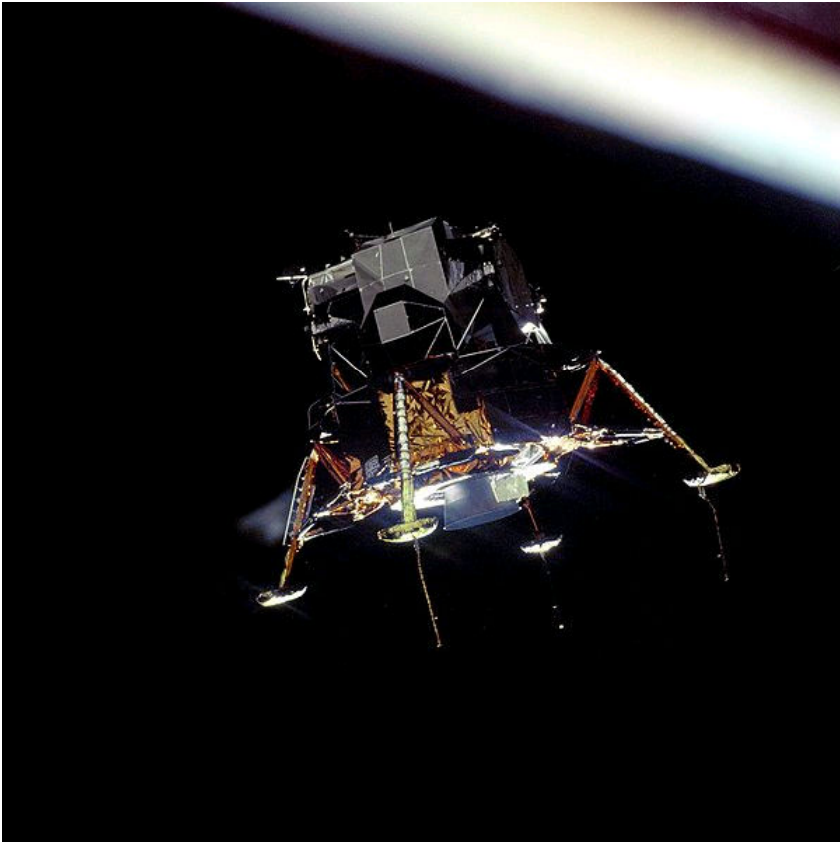


# Human Perception of Ambiguous Inertial Motion Cues

Neuroscience Laboratory  
Human Adaptation and Countermeasures Division  
NASA Johnson Space Center

Guan-Lu Zhang  
International Space University, MSS Candidate  
Co-Mentors: Dr. Scott Wood & Dr. Gilles Clément  
Faculty Advisory: Prof. John Farrow

# Manual Control Tasks

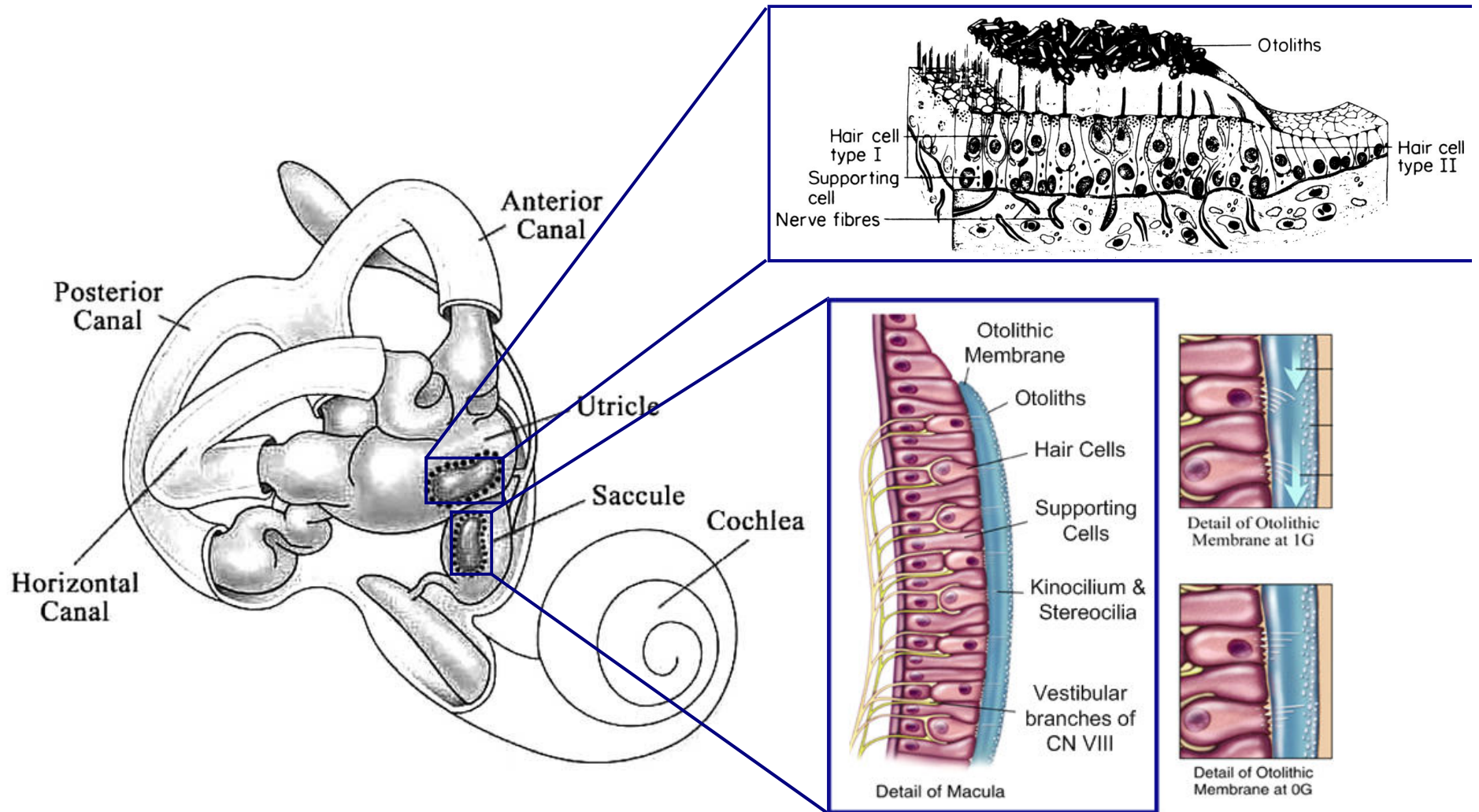


*Photos courtesy of NASA*

# Overview

- Vestibular Organ
- Ambiguous Motion
- Previous Work
- Hypothesis
- Tilt-Translation Sled
- Results
- Concluding Remarks

# The Human Vestibular Organ



# Ambiguous Motion Cues

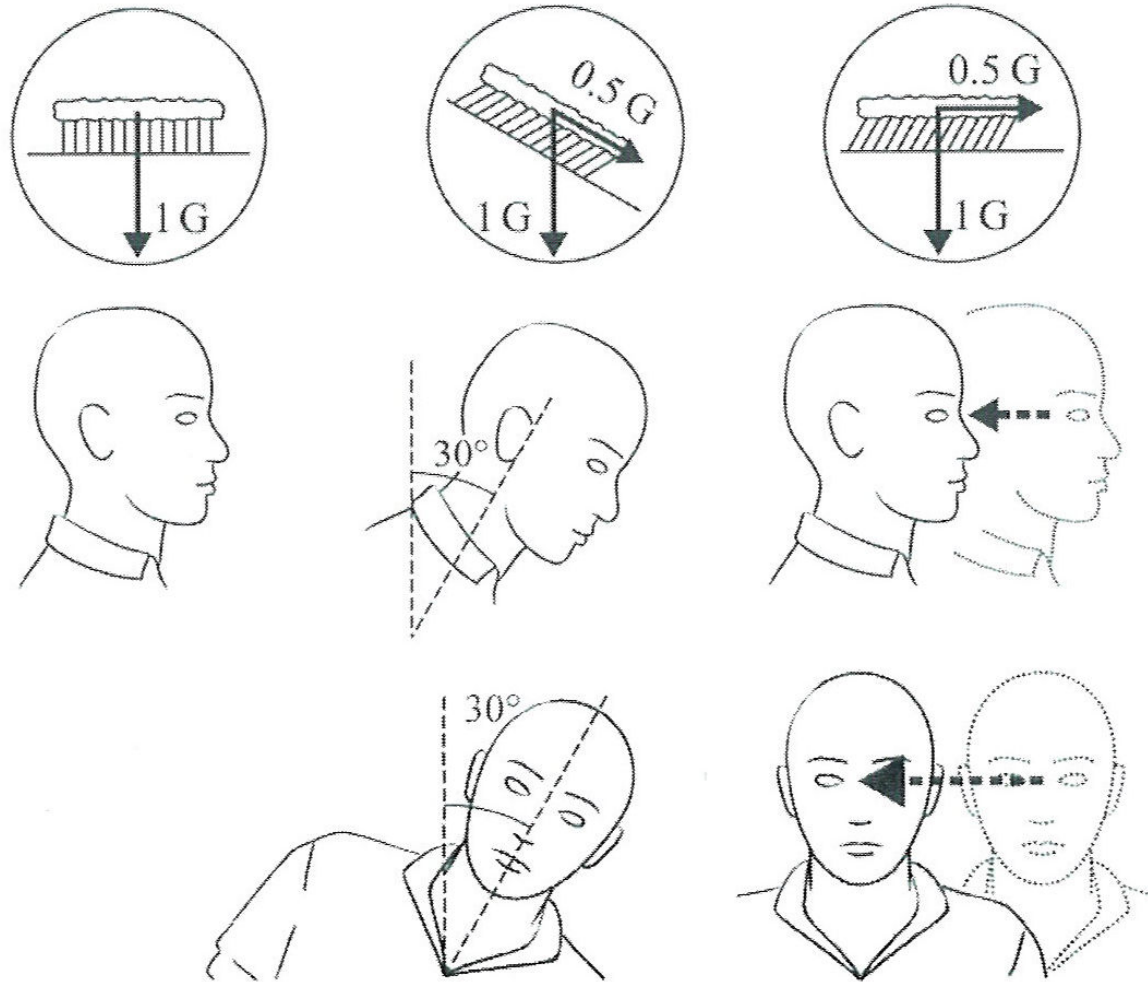


*Illustration courtesy of Philippe Tauzin*

# Previous Work

## Frequency Segregation

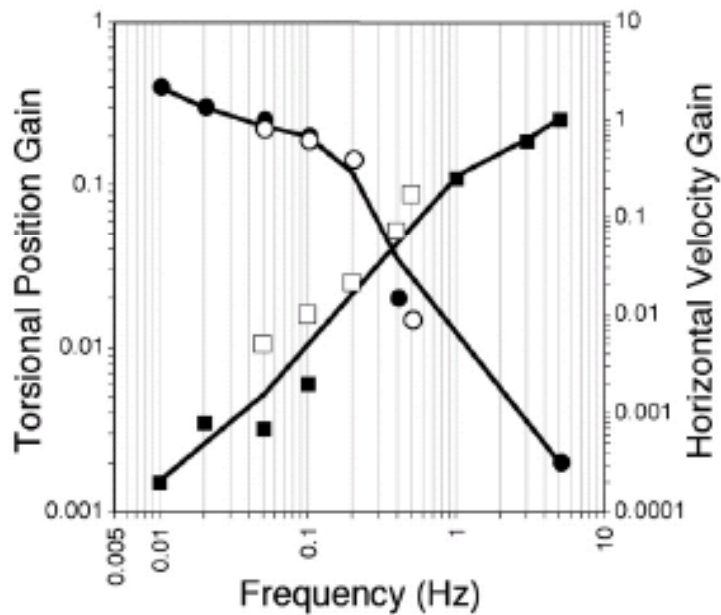


Figure courtesy of Clément & Reschke 2008

## Sensory Integration

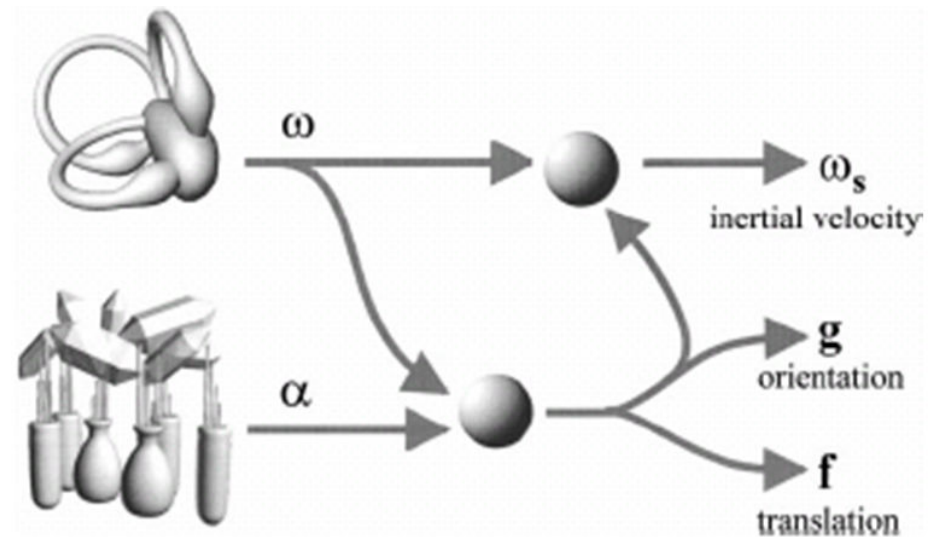


Figure courtesy of Angelaki 1999

# Previous Work

## Force Resolution

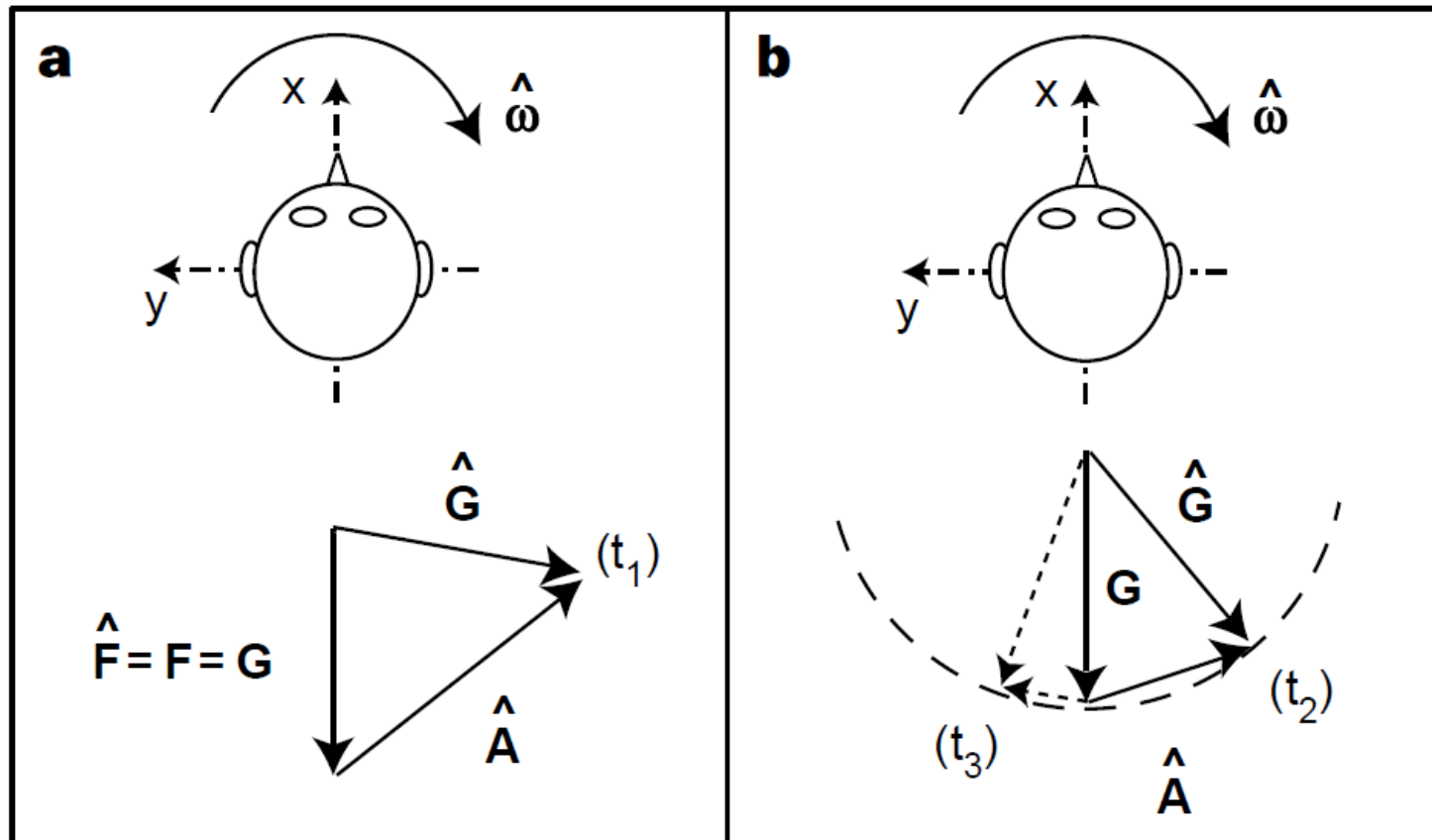
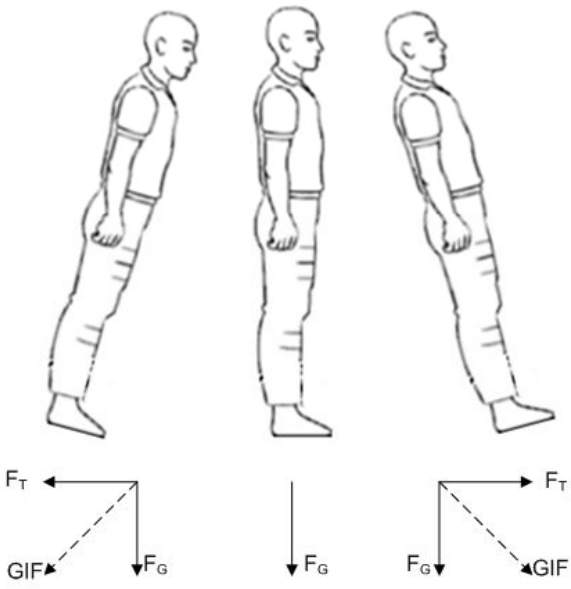
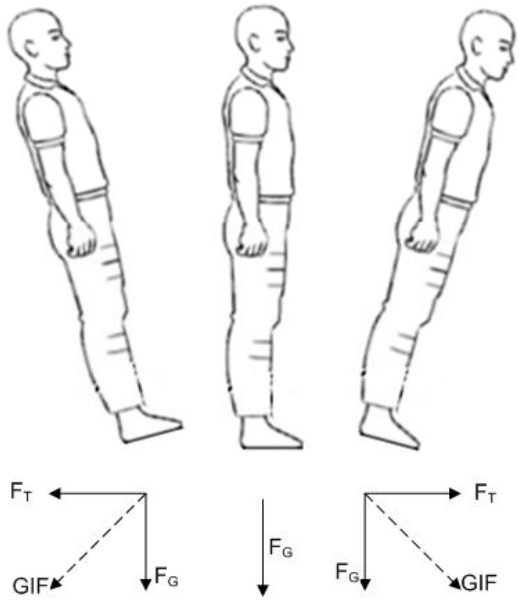


Figure adapted from Merfeld 1999

# Hypothesis

## Z-Axis Independent Gravitoinertial (ZIG) Motion

## Z-Axis Aligned Gravitoinertial (ZAG) Motion



**↑ Tilt**

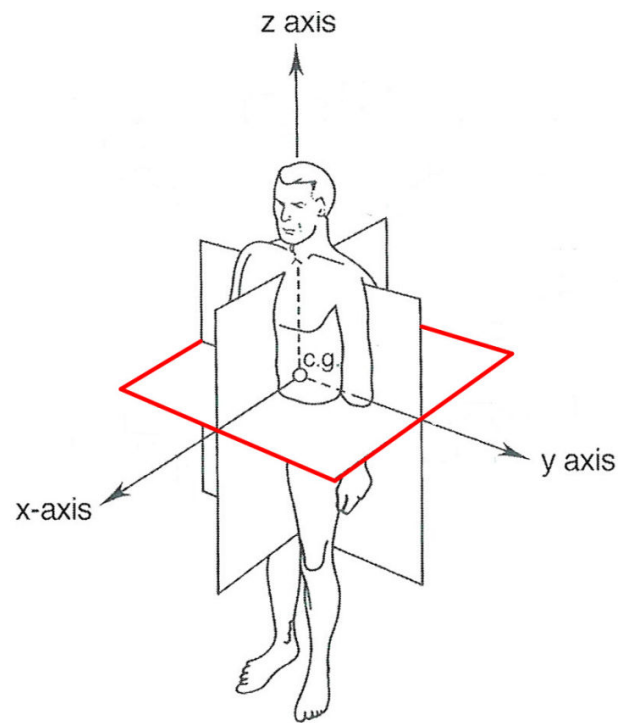
**↓ Tilt**

**↓ Translation**

**↑ Translation**

# Purpose of the Study

Characterize the human perception of ambiguous tilt and translation motion paradigms with varying phase and amplitude



# Tilt-Translation Sled



*Photos courtesy of Neuroscience Lab, NASA, JSC*

# Tilt-Only



# Translation-Only



# Z-Axis Independent Gravitoinertial (ZIG) Motion



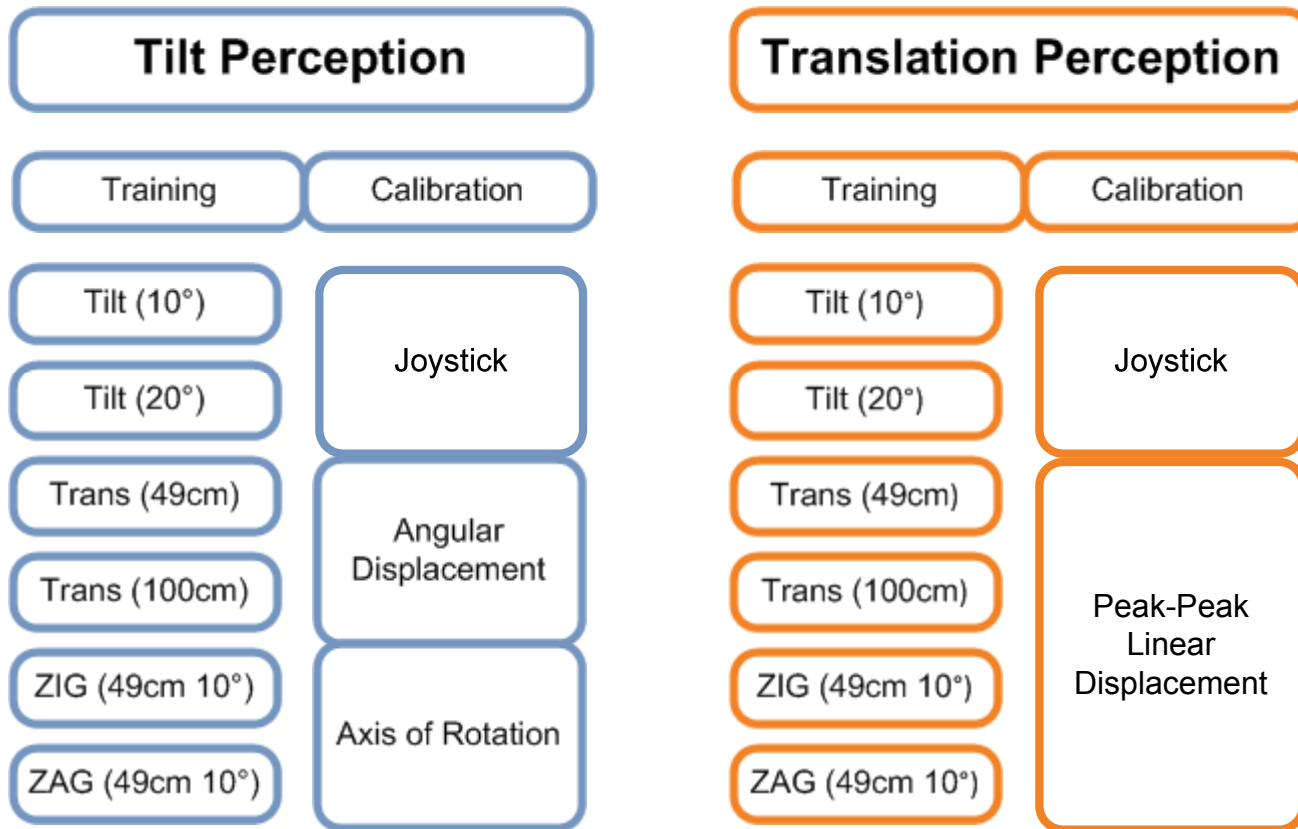
# Z-Axis Aligned Gravito inertial(ZAG) Motion



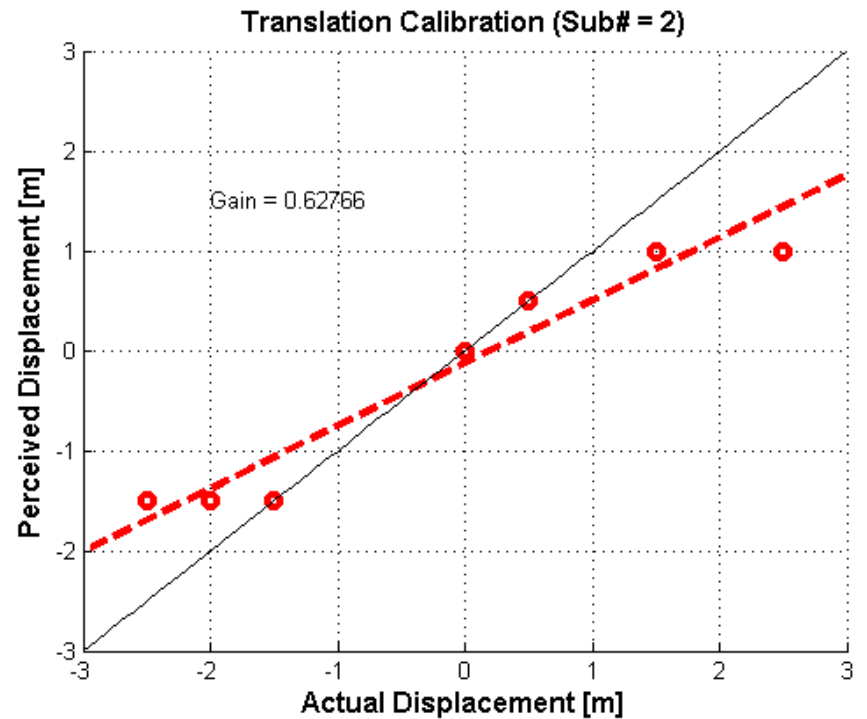
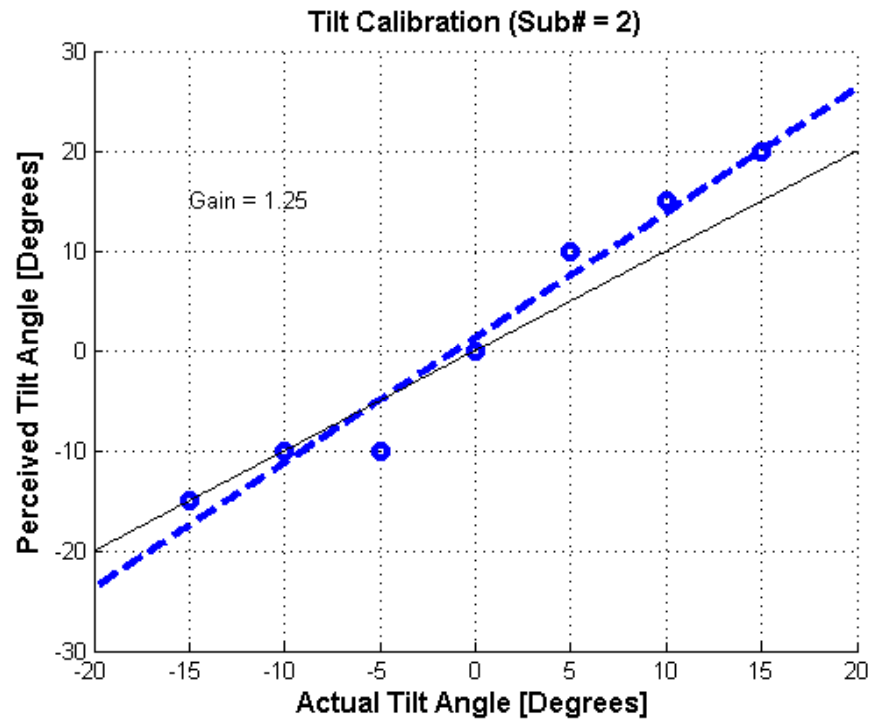
# Experimental Methods

- General public with healthy vestibular systems
- Flag subjects with symptoms of motion sickness ( $\geq 4$  on 0-10 nausea scale)
- Total subjects: 11/12

# Experimental Procedure

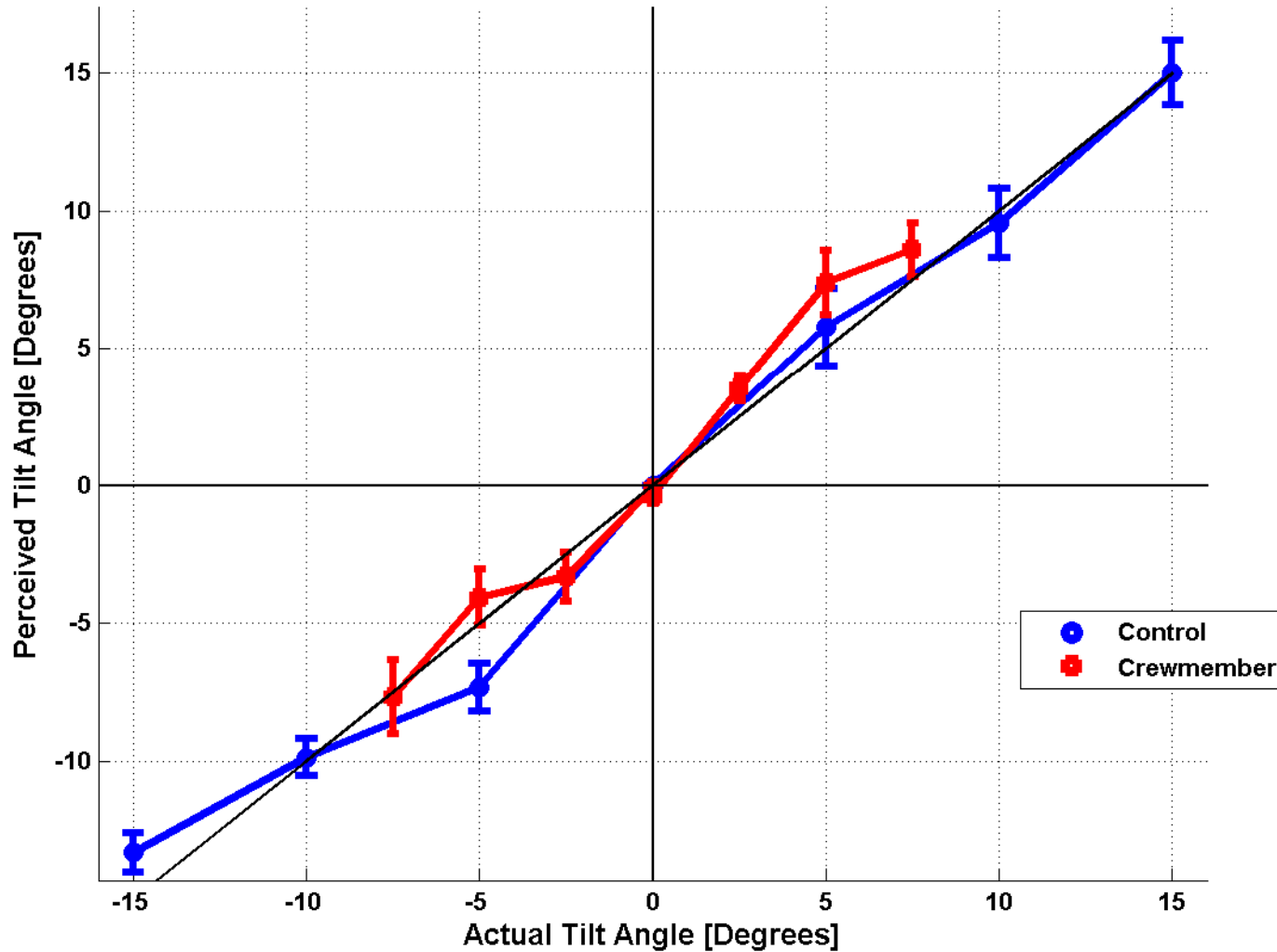


# Individual Calibrations

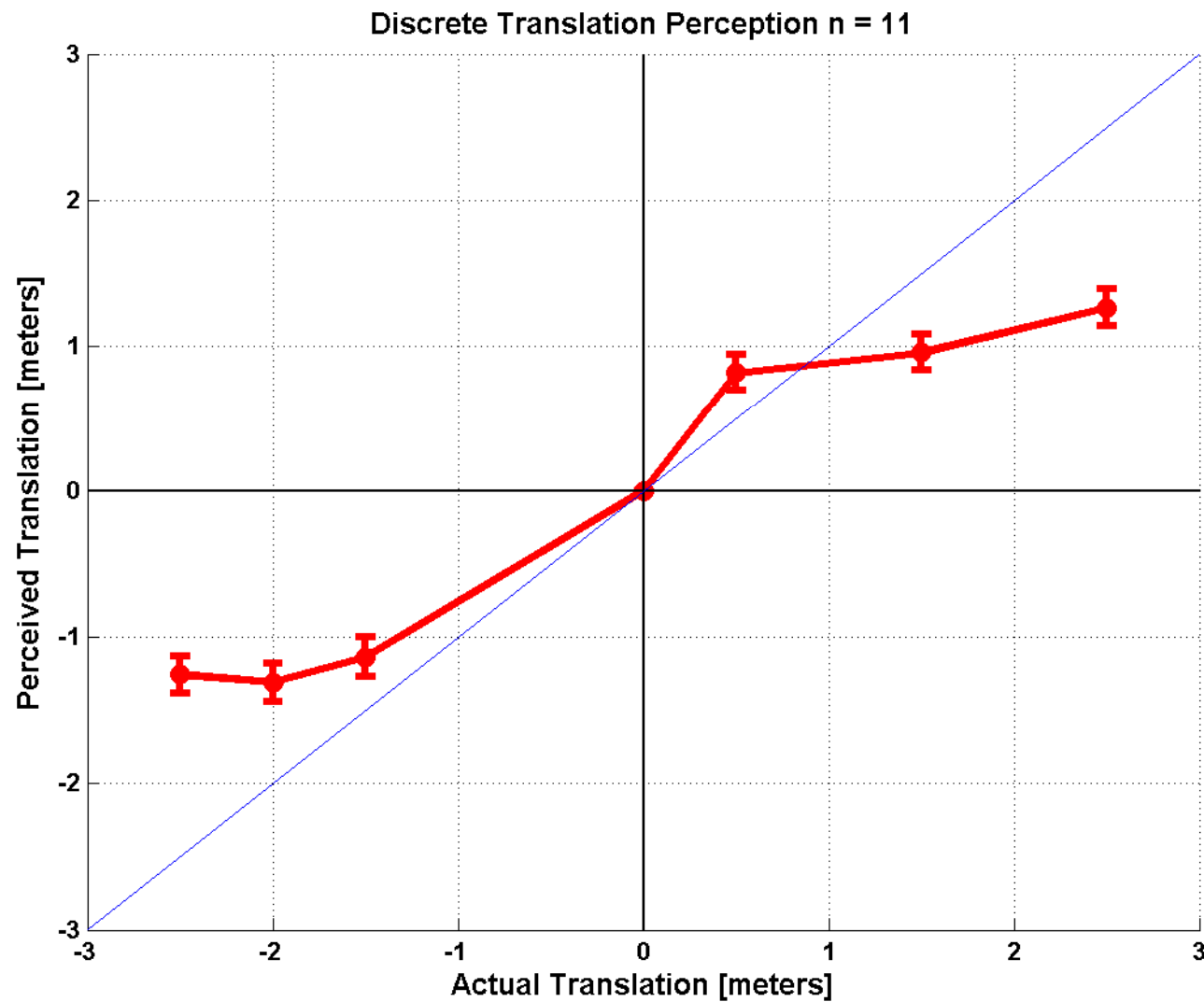


# Tilt Calibration

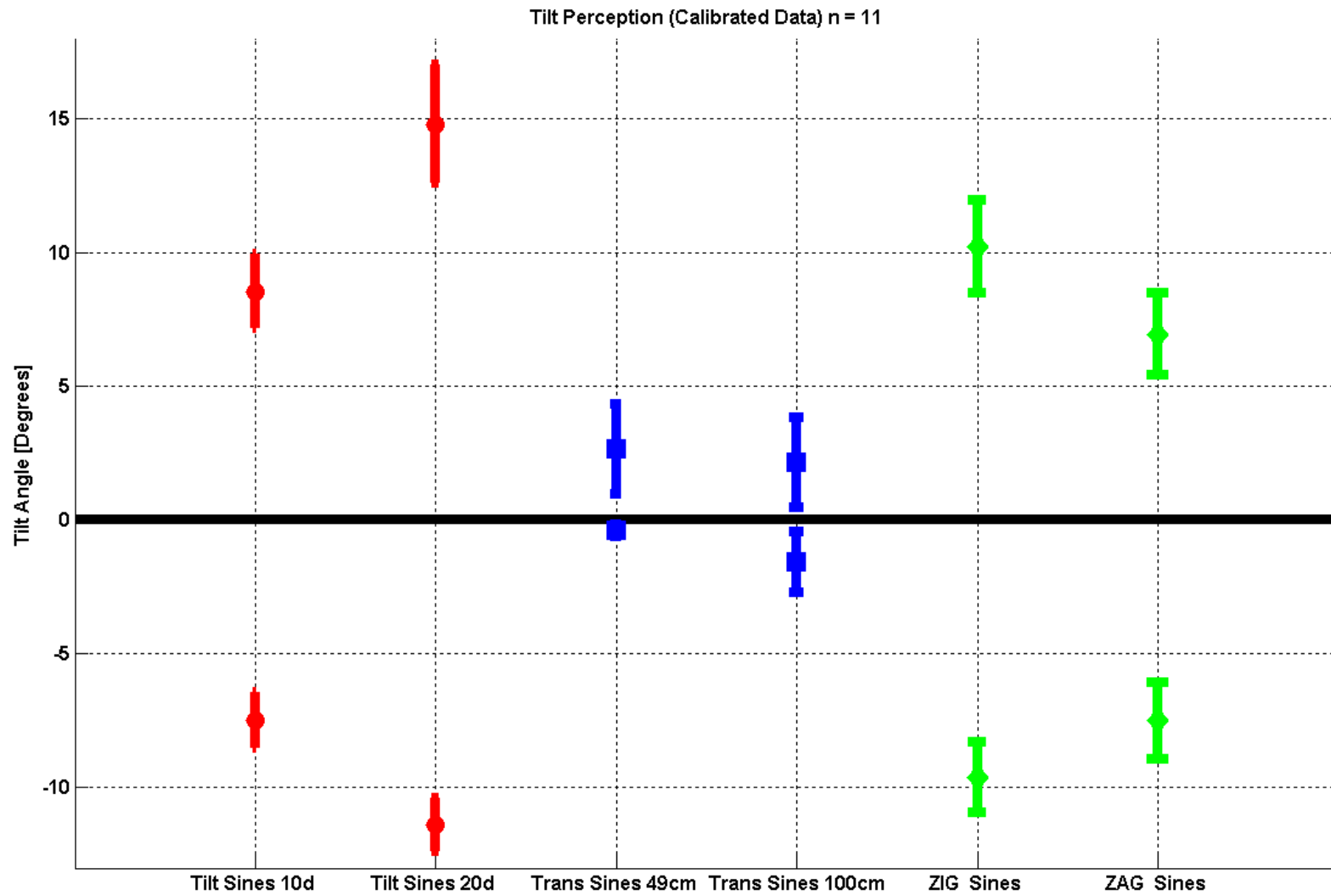
Static Tilt Perception: Control (n = 11) vs. Crewmember (n = 7)



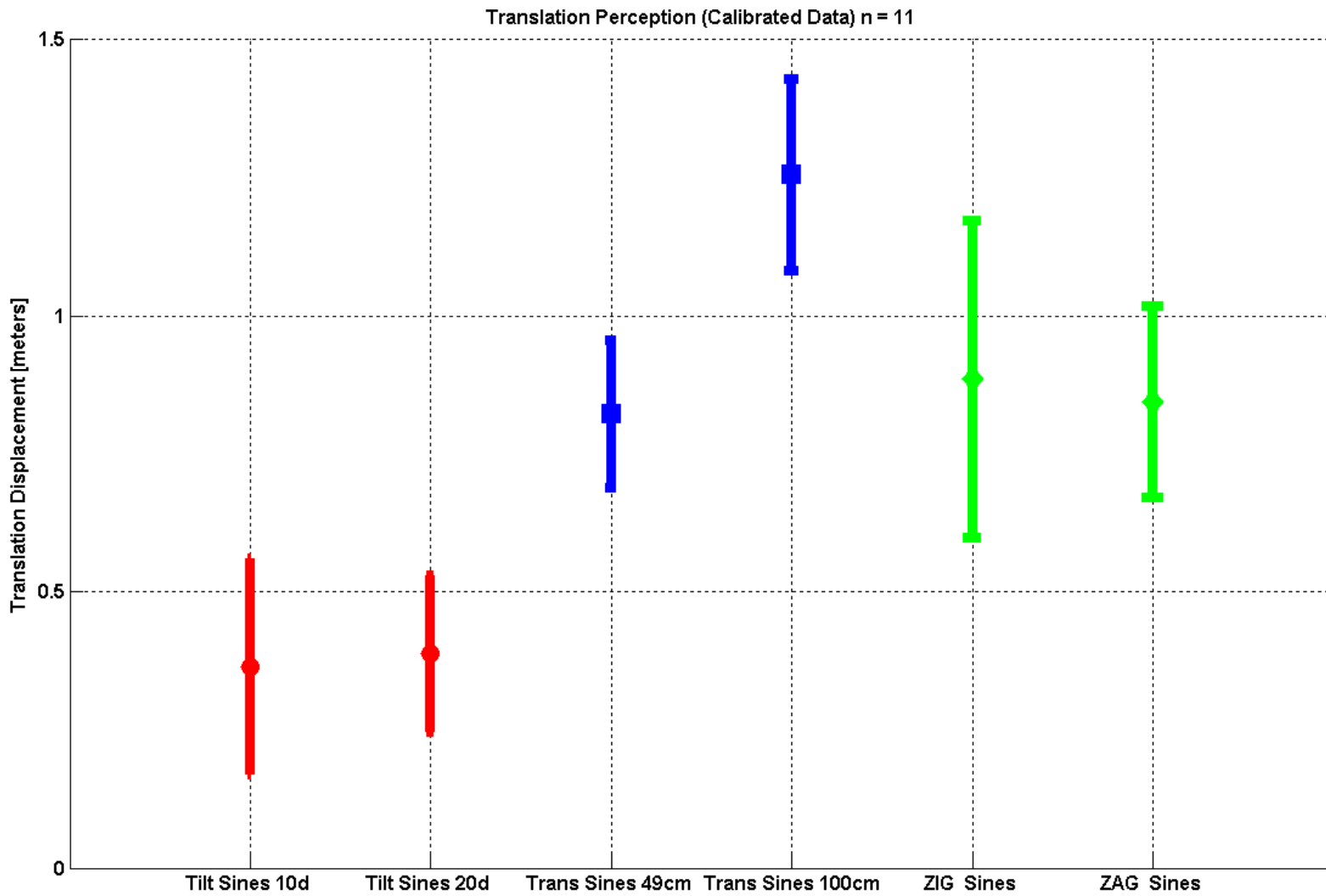
# Translation Calibration



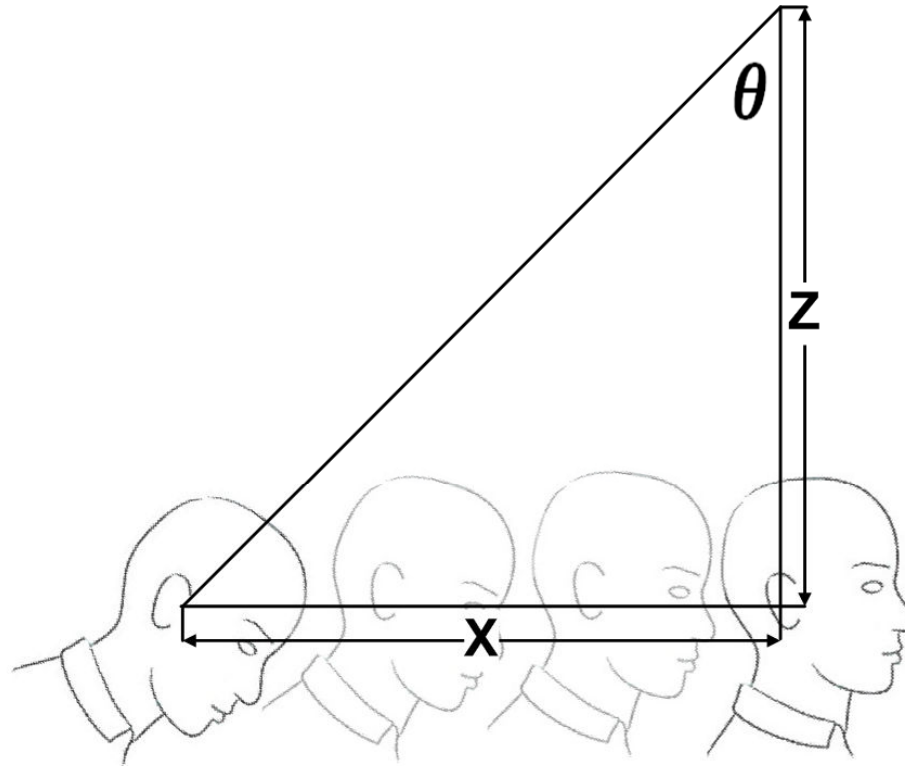
# Tilt Perception



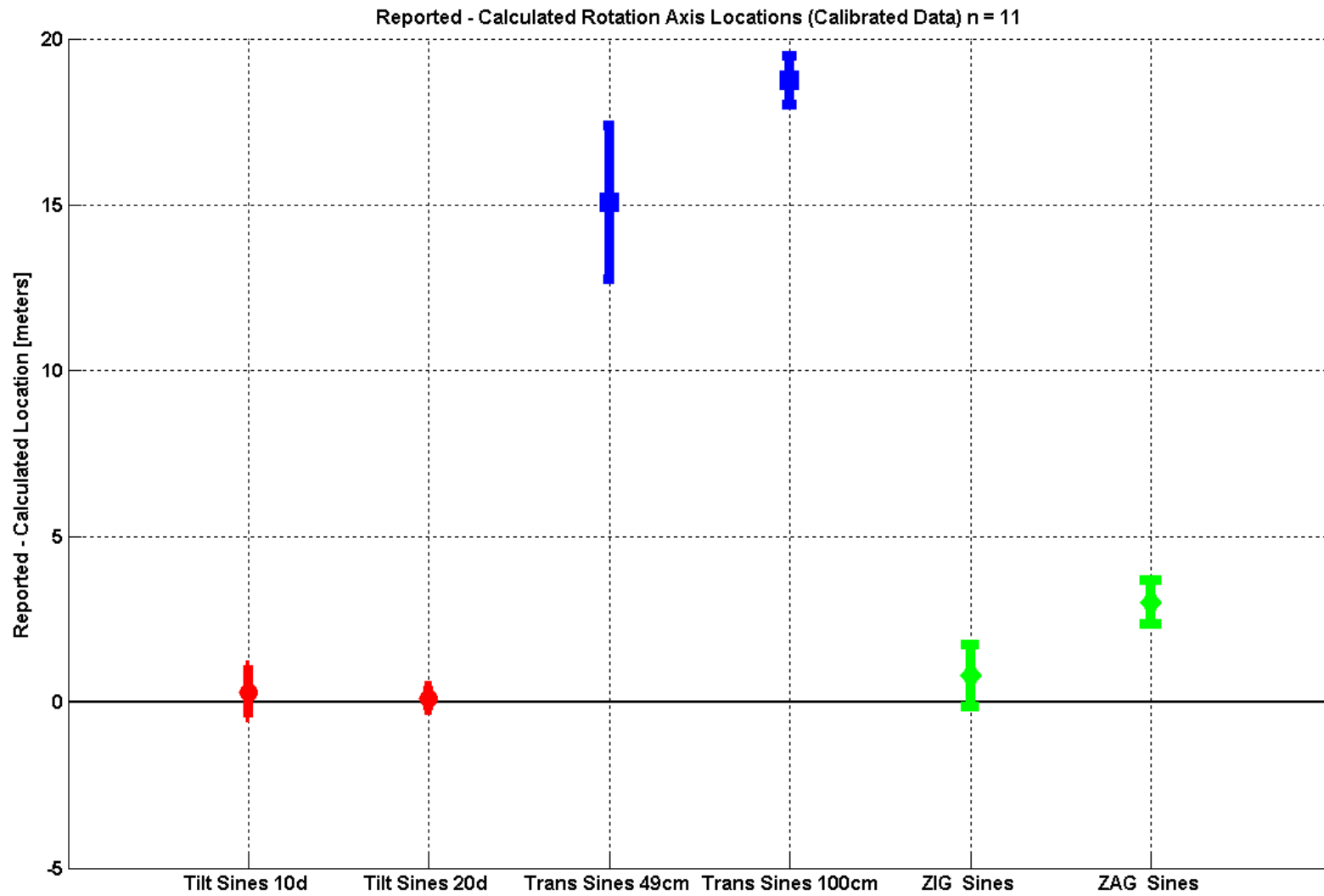
# Translation Perception



# Axis of Rotation



# Axis of Rotation



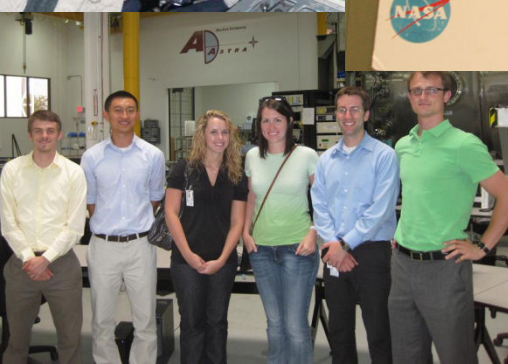
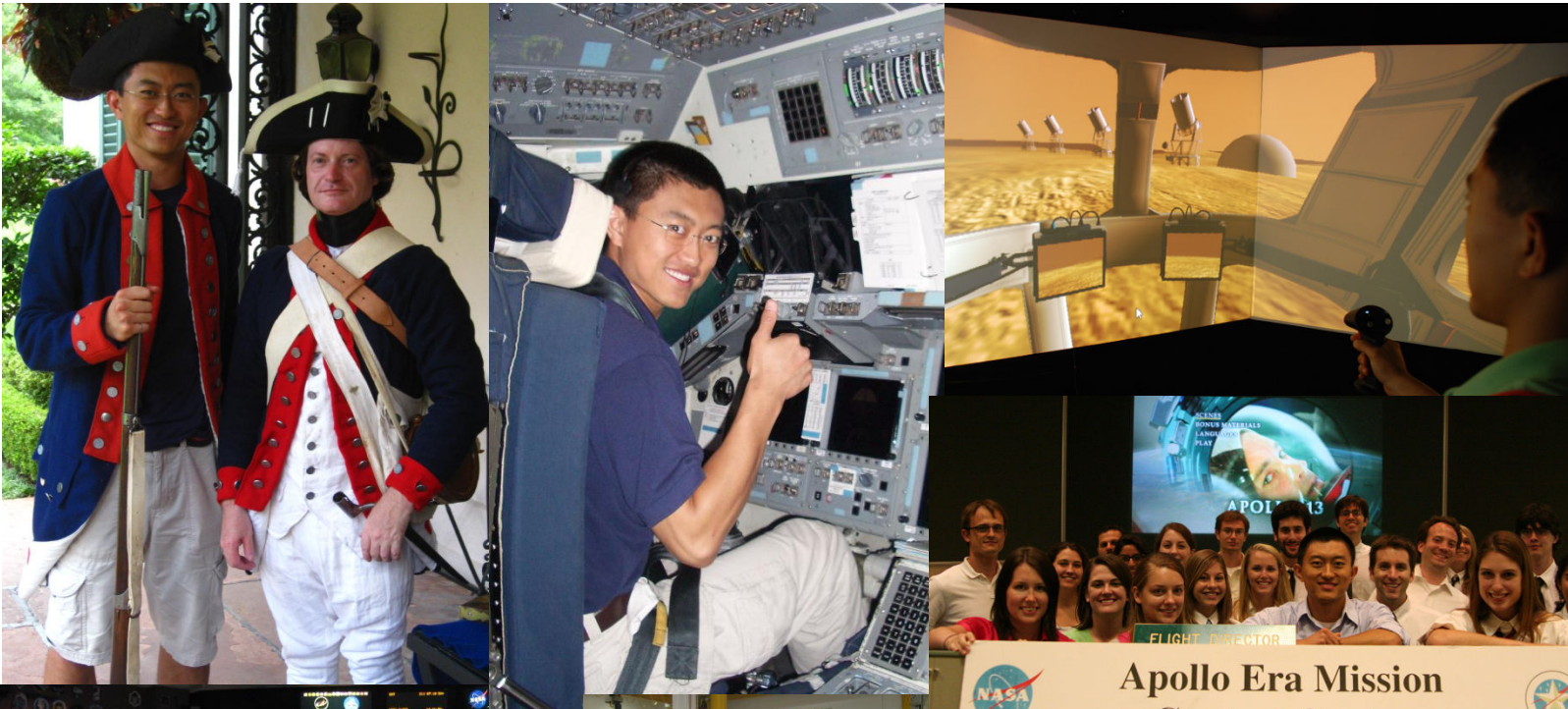
# Concluding Remarks

- Training in tilt is more effective than training in translation
- GIF resolution is inconclusive (ZIG vs. ZAG)

## Future Work:

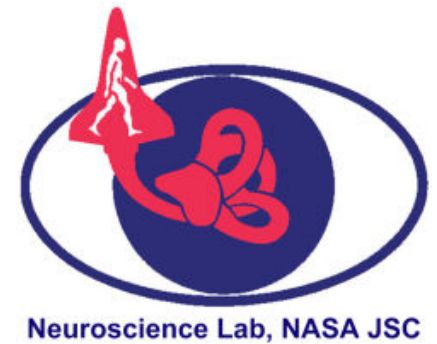
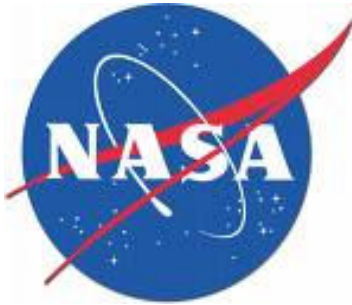
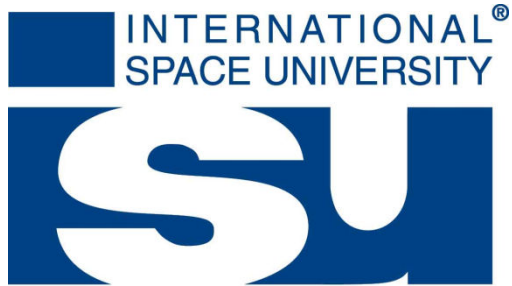
- Implement experiments on critical tracking
- Map perception deviations to tracking errors

# Good Times in Houston



# Acknowledgment

- Mentors: Scott & Gilles
- Co-pilot: Julie
- Technical help: Wally & Robert
- Roommate: Matthew
- Badging: Jan, Scott & Judy Hayes
- NASA insights: Elisa & Laura
- Too many others to thank



Thank you  
Questions & Comments?